CARL ZEISS
7082 Oberkochen
West Germany

Nomarski Differential Interference-Contrast Microscopy

Reprint

Collection of four articles from ZEISS Informations.

Author: Dr. Walter Lang,
scientific staff member of
CARL ZEISS, Oberkochen.

I. Fundamentals and experimental designs

Since 1965, CARL ZEISS of Oberkochen has been supplying interference-contrast equipment for transmitted light and since 1967 for reflected light, both based on suggestions by Professor *G. Nomarski*. This equipment was developed in close cooperation with *Nomarski* and has meanwhile proven superior results in the manifold uses of optical interference-contrast techniques.

The increasingly spreading acceptance and use of *Nomarski* differential interference-contrast microscopy call for a comprehensive description of this technique. This is part one of a paper on the subject and it deals with the physical principles of the method and the instrumentation developed for it. A second paper will discuss the formation and interpretation of the differential interference-contrast image. Both together will serve as a basis for a comparison of *Nomarski* differential interference-contrast with phase-contrast, which will follow in a third paper. Finally, a fourth paper will deal with the applications of *Nomarski* differential interference-contrast. For easier comprehension we have avoided going into mathematical explanations. However, numerous references are given for readers who wish to pursue the study of the subject further.

First, the principle of interference-contrast microscopy will be explained. Then the most notable differences between the *Jamin-Lebedeff* and the *Nomarski* interference methods will be discussed. This will offer an opportunity to give a summary of the most important terms used in crystal optics and required to understand how the two methods

Fig. 1: Interference micrographs of polished chrome-nickel steel showing increasing spacing of interference fringes (see 27) produced by tilting a plane-parallel plate in the light path (36).

1

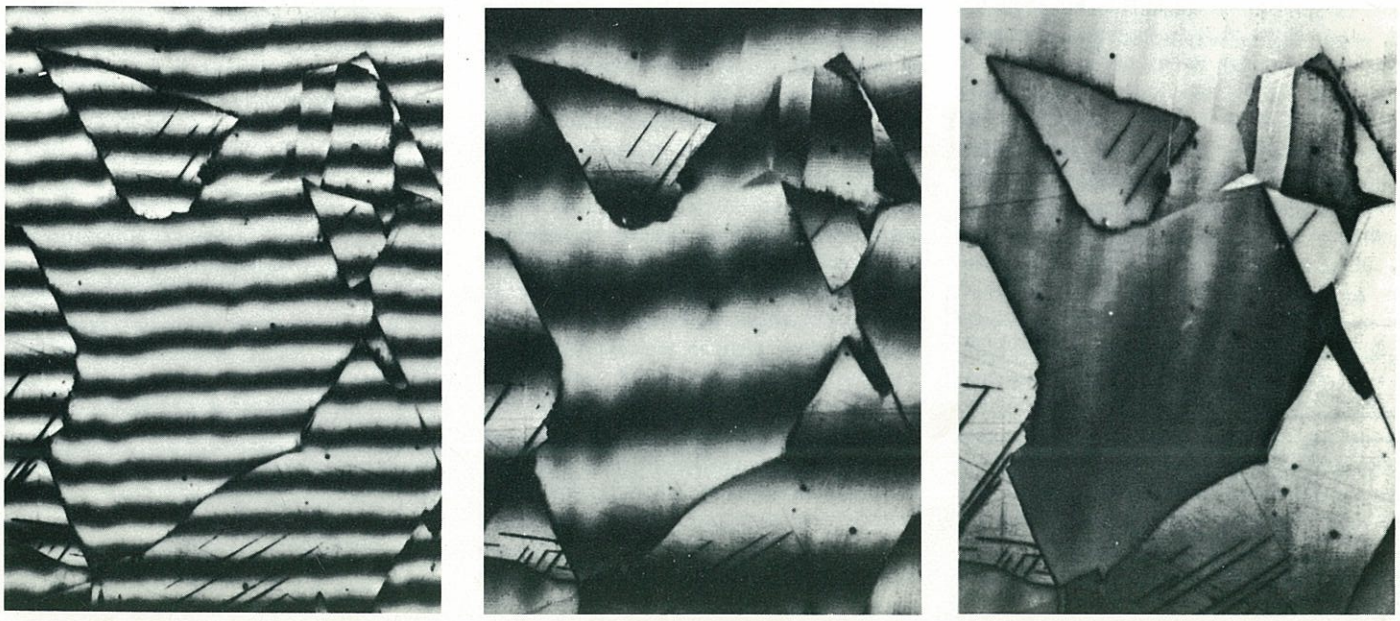

operate. The design of the *Nomarski* interference-contrast microscope for transmitted light is described for two different techniques: one for double-beam interference microscopy, the other for the compensation of interference fringes. Both are also applicable to describe the equipment for reflected light.

1. Basic principles of interference-contrast microscopy

If in an interference microscope the distance between fringes (and thus also the width of the fringes) is made so wide that one fringe covers the entire field of view, we speak of an infinite spreading of that particular interference fringe, or of interference contrast. Thereby the area of interest in a specimen is rendered visible by interference-contrast (6, 7, 8, 18, 23, 30). This can be explained with the aid of the micrographs shown in Fig. 1, which were taken by reflected light under the Interference Microscope made by CARL ZEISS, Oberkochen. This instrument, as a rule, is set in such a way that interference fringes are visible in the field of view. Under reflected light, the distance between fringes corresponds to half the wavelength of the monochromatic light used. Path differences, expressed in fractions or multiples of half a wavelength of the light used and produced by irregularities in the surface structure of the specimen, result in a displacement of the fringes. The amount of fringe shift is directly proportional to the path difference.

In the micrograph to the left in Fig. 1 the fringe spacing is very narrow; consequently, the fringe shift is also small, but the fringes are well defined and have relatively sharp contours. The micrograph in the center illustrates the transitional stage between finite and infinite fringe spacing: only five interference fringes can be seen in the field of view (as compared to 14 in the previous micrograph). Here, too, the path difference or fringe shift is expressed as fractions of half a wavelength of the light used. However, it is also obvious that the edges of the fringes are more or less "blurred". In the micrograph to the right, finally, the distance between two neighboring fringes is greater than the field of view. Here we speak of an infinitely wide distance between fringes or – in accordance with the definition given above – of interference contrast. A comparison with the other two micrographs clearly shows that in the case of interference contrast path differences are transformed into differences of brightness. This enhances the clarity of the microscopic image which appears to be almost three-dimensional, due to a certain shadow effect. On the other hand, it becomes also obvious that path differences can no longer be easily determined since no measurable fringe shift exists in interference contrast.

2. Operating principle of ZEISS double-beam interference microscopes

CARL ZEISS of Oberkochen, West Germany, produces three different double-beam interference microscopes: the *Michelson*, *Jamin-Lebedeff* and *Nomarski* types. The *Michelson*, which was used to take the micrographs shown in Fig. 1, is characteristic for the wide separation of the specimen and reference beams[1], which can reach an order of magnitude of up to a few centimeters. In the *Jamin-Lebedeff* interference microscope, the lateral separation of the reference beam in relation to the specimen beam is considerably smaller, namely a few millimeters (see below). Finally, in the *Nomarski* interference microscope, the lateral separation of the two beams is only a few microns, i. e., it is slightly smaller than the resolving power of the microscope. In this case we speak of differential splitting of beams.

In double-beam interference microscopes the magnitude of beam splitting is of great importance for the interference image and offers another classification of double-beam microscopes: in the case of the *Michelson*-type microscope we can always assume that the reference beam is not affected by the specimen. In interference microscopes of the *Jamin-Lebedeff* type, the reference beam is only then not influenced by the specimen if the specimen under examination is smaller than the distance between the two beams. However, if we leave to deal with a differential splitting of beams, as is the case in the *Nomarski* interference microscope, the terms "specimen beam" and "reference beam" have no meaning since both beams pass through the microscopic specimen. In other words, with differential beam splitting both beams are influenced by the specimen – a fact that must definitely be taken into account when interpreting the interference image.

In addition to the aforementioned differences existing in the double-beam interference microscopes, there is another distinguishing characteristic, that of splitting and recombining the beam. In the interference microscope of the *Michelson* type a beam-splitting prism is used. (For further details, see 11, 13, 16, 17, 28, 35, 36, 37, 40 and 41). In the *Jamin-Lebedeff* and *Nomarski* double-beam interference microscopes, on the other hand, the beams are split and recombined by birefringent crystals. Birefringent or doubly refracting crystals (3, 4, 23, 34) are crystals which split an incident light wave into two components which are plane-polarized and whose vibration planes run perpendicular to each other. Fig. 2 may serve as an explanation. It also illustrates the principle of wave splitting in the *Jamin-Lebedeff* microscope. Let us assume that a light wave, of which the diagram shows only the axis, hits a plane-parallel calcite plate perpendicularly. Furthermore, we assume that the incident wave is plane-polarized and its vibration plane is inclined by 45° to the plane of the diagram. The optic axis[2] of the calcite plate – marked by the double arrow – runs parallel to the plane of the diagram. As the beam enters the crystal, the wave is split into two parts, the axes of which are entered in the diagram as a principal section[3]. The so-called ordinary wave is transmitted by the crystal without any deflection. The so-called extraordinary wave is deflected to one side, in spite of its vertical (90°) incidence on the plane-parallel plate. It emerges from the crystal parallel to the axis of the ordinary wave. If the direction in which the crystal is cut is known, the separation between the two waves is a function of the thickness of the crystal plate. In the case of the ZEISS *Jamin-Lebedeff* transmitted-light interference equipment it amounts to minimum 0.05 mm (Achromat Pol Int., 100 x, 1.0 N. A., oil) and maximum 0.5 mm (Achromat Pol Int., 10 x, 0.22 N. A.). As is evident from Fig. 2, a birefringent plate is characterized by another feature in addition to lateral beam splitting. The plane-polarized light wave which hits the crystal and whose vibration direction is offset by 45° to the plane of the diagram, is split into two plane-polarized components. The vibration direction of the ordinary wave is perpendicular to the plane of the diagram, while the vibration direction of the extraordinary wave coincides with the plane of the diagram. This is a fact which must be taken into account in the design of the *Jamin-Lebedeff* interference microscope, because, after recombination, the two coherent bundles can only interfere and produce an interference image, if the vibration directions of the two plane-polarized waves lie in one and the same plane[4].

Similar considerations also apply to the *Nomarski* differential interference microscope. They are of decisive importance not only for the formation, but also for the interpretation of the interference image.

---

[1] By specimen or measuring beam we understand the bundle of coherent light which passes through the specimen. The second coherent bundle, called reference or comparison beam, does not pass through the specimen but bypasses it.

[2] The optic axis of a birefringent crystal indicates the direction in which the ordinary and extraordinary waves coincide. This direction, in which the crystal behaves like an isotropic, i. e., not birefringent medium, is also called the isotropic axis. In the case of calcite and quartz it is identical with the optic axis of the crystal. Crystals which have only a single optic axis, e. g., calcite or quartz, are called uniaxial crystals.

[3] Any plane through the crystallographic axis is a principal section of a crystal.
(Following general parlance, the term "beam" taken from geometrical optics is here and in the following frequently used instead of the more appropriate terms "bundle of rays" or "light wave".)

[4] The term "plane of polarization" (plane perpendicular to the vibration direction of the electric vector) used in earlier literature can be dispensed with and is not used in this paper.

2

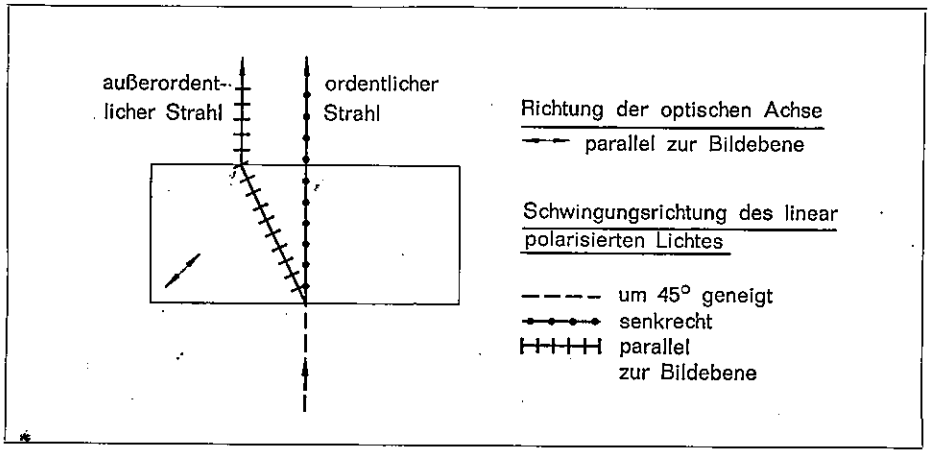

Fig. 2: Beam path in the principal section of a birefringent plate.
(außerordentlicher Strahl = Extraordinary ray, ordentlicher Strahl = Ordinary ray, Richtung der optischen Achse = Direction of optic axis, parallel zur Bildebene = parallel to image plane, Schwingungsrichtung des linear polarisierten Lichtes = Vibration direction of plane-polarized light, um 45° geneigt = inclined by 45°, senkrecht = perpendicular, parallel zur Bildebene = parallel to image plane)

3

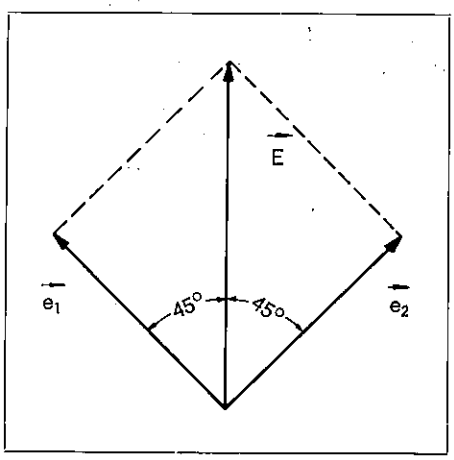

Fig. 3: Splitting the vector $\vec{E}$ into $\vec{e_1}$ and $\vec{e_2}$, the last two at right angles to each other.

Therefore, the splitting of a plane-polarized wave into two plane-polarized components of different vibration directions will be discussed in greater detail (see also 6, 21, 22, 34). The opposite process, namely the recombining of two plane-polarized components into a plane-polarized wave, will be dealt with in connection with the interpretation of the differential-interference image.

The vibration direction of a plane-polarized light wave is identical with the plane in which the vector of the electric field strength $\vec{E}$ vibrates. In accordance with the rules governing the calculus of vectors, $\vec{E}$ can be split up into two vectors, $\vec{e_1}$ and $\vec{e_2}$, which are at right angles to each other and each of which forms an angle of 45° with $\vec{E}$ (Fig. 3).

If we apply this formalism to a plane-polarized light wave, the electric vector of which changes sinusoidally with time, we obtain the diagrammatic representation in Fig. 4: it shows a sine wave (center curve) proceeding from the left foreground to the right background; the vibrations represented by the two inclined curves are equivalent to it.

The form of representation chosen in Fig. 5 is particularly advantageous for interpreting the differential interference-contrast image. It summarizes the most essential results of Figs. 3 and 4. Let W in (a) be a plane-polarized wave normal to the plane of the diagram. Following the scheme of Fig. 3, this wave with the vectors $\vec{E}$ and $\vec{E}'$ (b) can be split into the tho components w_1 and w_2 with the vectors $\vec{e_1}$, $\vec{e_1}'$ and $\vec{e_2}$, $\vec{e_2}'$. In (c) the vibration plane of the wave W coincides with the plane of the diagram.

As was mentioned above, a strong lateral beam-splitting effect is achieved in the *Jamin-Lebedeff* interference microscope with the aid of a birefringent plane-parallel plate. (Questions of the beam recombination and compensation cannot be discussed here. For more information interested readers are referred to the pertinent literature: 9, 10, 14, 20, 23. For numerous references, see 25).

If a so-called *Wollaston* prism is used as a beam splitter instead of a birefringent plane-parallel plate, the beam splitting that results will not be lateral but angular (Fig. 6). A *Wollaston* prism consists of two prisms cemented together and made of birefringent, uniaxial material (preferably quartz or calcite). The optic axes of the two prisms are at right angles to each other. If a plane-polarized bundle of light (vibration plane inclined by 45° to the plane of the drawing) hits the *Wollaston* prism perpendicularly, as is shown in Fig. 6, it will be split into two plane-polarized waves in the lower prism, the vibration planes of which each make an angle of 45° with the incident wave (see Figs. 3 and 5). At the cemented surface of the *Wollaston* prism the two component waves are deflected in two directions at a certain, relatively small angle. The ordinary wave[5] is deflected towards the base of the upper prism, while the extraordinary wave[5] is deviated towards the edge of the upper prism. The two component beams encounter different indices of refraction so that the wavefronts travel with different speed.

3. Double-beam interference-contrast microscope with two Wollaston prisms

On the basis of the explanatory remarks in the previous section, the design of a double-beam interference-contrast microscope can be easily explained with the aid of Fig. 7 (see also 5, 8, 30, 31, 32). The unpolarized light emerging from the field diaphragm is plane-polarized by the polarizer and strikes the first *Wollaston* prism. As was explained above, angular beam splitting occurs at the cemented surface of this prism. (For greater clarity, one of the prism segments is dotted). If the center plane of the *Wollaston* prism lies in the lamp-side focal plane of the condenser, the two beams will travel along parallel paths, slightly separated laterally in relation to each other, after they emerge from the condenser. They pass through the specimen and the microscope objective and converge in the image-side focal plane of the microscope objective. This is where a second *Wollaston* prism is located, which has the same dimensions and optical properties as the first one. Together with the microscope objective the second prism recombines the two beams. After emerging from the second *Wollaston* prism, the two components once more form a single beam, but they are still plane-polarized and their vibration planes are at right angles to each other. In order to enable the two waves to produce the desired interference effect in the intermediate image plane, their vibration planes must coincide. This can be achieved by inserting an analyzer into the light path. The diagram in Fig. 5 shows the two components now recombined to form a single,

[5] The ordinary wave is the component vibration perpendicular to the plane of the crystal's principal section. Conversely, an extraordinary wave vibrates parallel to the plane of the principal section. Since the Wollaston prism is composed of two prism elements, the optic axes of which form an angle of 90°, it has two different, mutually perpendicular principal planes. Since, moreover, the vibration direction of the two components is fully preserved on the way from the lower to the upper prism, the ordinary wave of the lower prism becomes the extraordinary wave in the upper prism, while the extraordinary wave of the lower becomes the ordinary wave in the upper prism.

Fig. 4: Splitting a plane-polarized wave (central curve) into two plane-polarized components, at right angles to each other.

Fig. 5 a): Plane-polarized wave W with vibration plane, at right angles to plane of drawing; b) Splitting of the wave W into two plane-polarized waves w_1 and w_2; c) Same as b), but traveling direction of wave W identical with plane of diagram.

Fig. 6: Angular splitting of a plane-polarized light wave with the aid of a Wollaston prism. (For greater clarity, the angular splitting has been exaggerated. The term "image plane" stands for the plane of the diagram and not the intermediate image plane of the microscope.)

(außerordentlicher Strahl = Extraordinary ray, ordentlicher Strahl = Ordinary ray, Richtung der optischen Achse = Direction of optic axis, parallel = parallel, senkrecht zur Bildebene = perpendicular to image plane, Schwingungsebene des Lichtes = Vibration direction of light, unter 45° geneigt = inclined by 45°, senkrecht = perpendicular, parallel zur Bildebene = parallel to image plane)

4

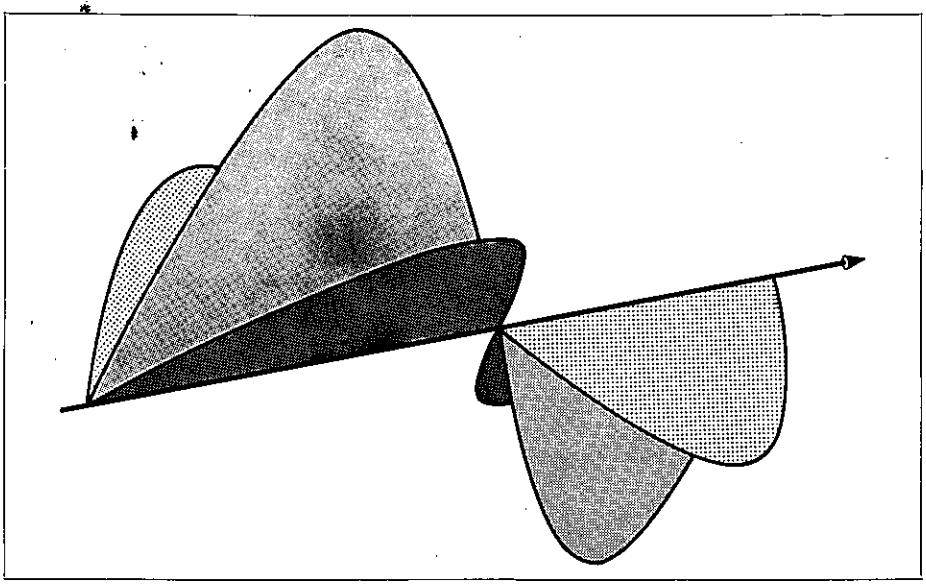

5

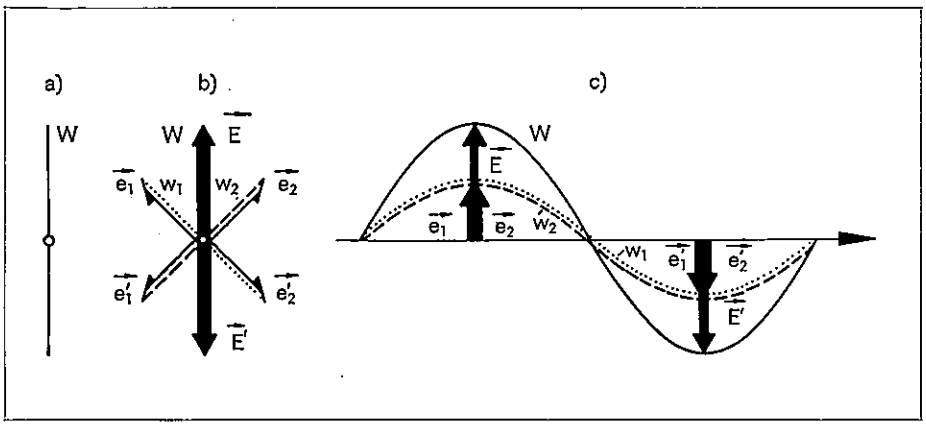

6

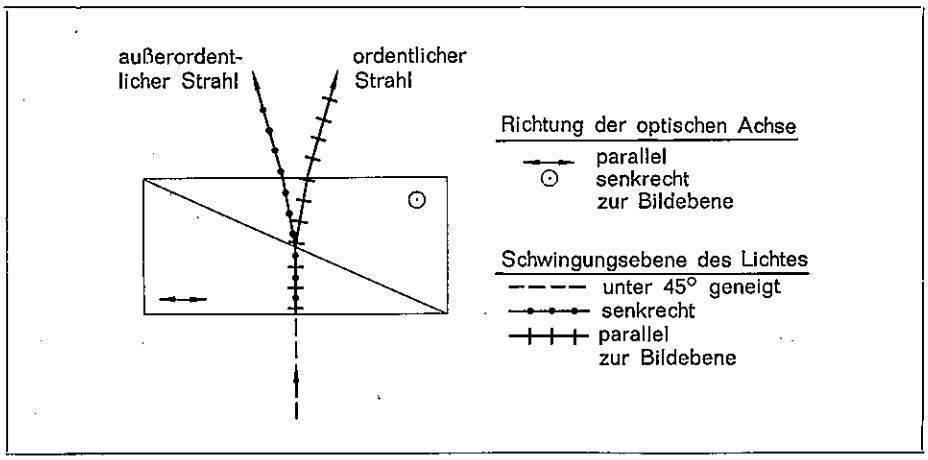

plane-polarized wave that is capable of interference. The resulting interference intermediate image can be viewed through the eyepiece in the conventional manner.

While Fig. 7 merely shows the principle of beam splitting and recombination, diagram Fig. 8 also indicates the vibration directions of the polarized components at different points along their path. Fig. 8 shows only the axes of the light beams. The polarizer is oriented in such a way that the natural light emerging from the field diaphragm (not shown) is plane-polarized and its vibration plane is inclined by 45° to the plane of the diagram. In the lower part of the *Wollaston* prism, the polarized wave entering it is split into two plane-polarized components. The vibration of the dotted beam is perpendicular to the plane of the diagram, that of the cross-lined beam is parallel to the plane of the diagram. Both beam components pass through the specimen parallel to each other and only a short distance apart.

Above the specimen plane, the two beam components are recombined with the aid of the microscope objective and the second *Wollaston* prism. It becomes obvious that the condenser with the first *Wollaston* prism and the objective with the second *Wollaston* prism are functionally correlated. The analyzer is oriented so as to form an angle of 45° with the vibration plane of each of the entering waves. In accordance with Figs. 4 and 5 this ensures that both beam components act with the same intensity. What happens when the analyzer forms an angle other than 45° with the two beam components will be discussed in detail in connection with the interpretation of the differential interference-contrast image.

In the equipment for transmitted light, two *Wollaston* prisms are needed for beam splitting and recombining, whereas only one Wollaston prism is required for a reflected-light setup, since the light passes through the prism twice in opposite directions (30, 31, 32). The splitting of the beam when it passes through the prism the first time is cancelled out when it passes the prism the second time. In other words, when the beam travels the first time through the prism the reflected-light objective and the *Wollaston* prism act in the same manner as the condenser and the first *Wollaston* prism of the transmitted-light setup illustrated in Figs. 7 and 8, while when it travels through the prism the second time, these components correspond to the objective and the second *Wollaston* prism in those figures. This is indicated by the diagram in Fig. 9: the beam that is plane-polarized by the polarizer is deflected to the *Wollaston* prism by a half-silvered mirror. The two beam components emerge from the reflected-light objective parallel to each other and with a slight lateral separation. The beams reflected by the specimen are then recombined with the aid of the objective and the *Wollaston* prism,

7

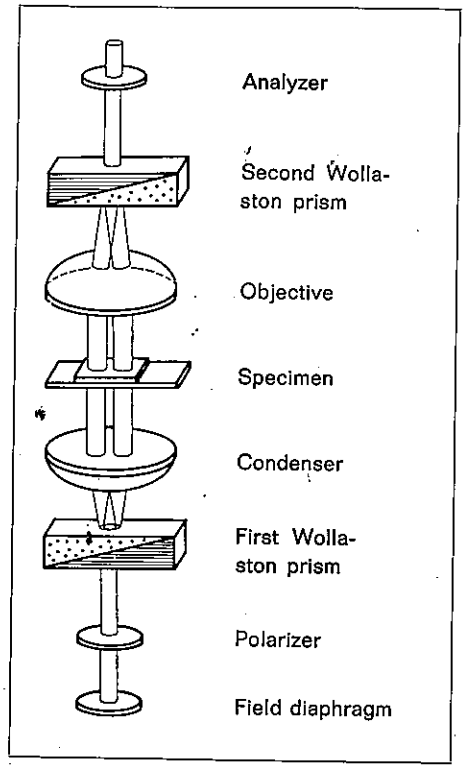

Fig. 7: Diagrammatic representation of a double-beam interference-contrast microscope as suggested by Smith, with two Wollaston prisms.

8

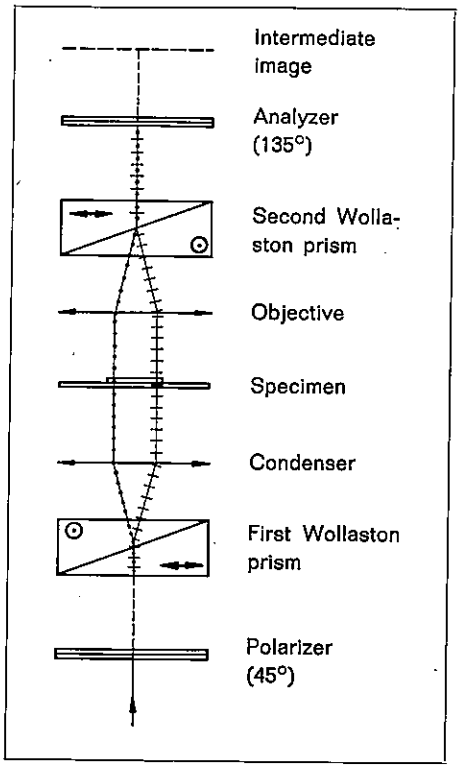

Fig. 8: Principle of a double-beam interference-contrast microscope with two Wollaston prisms. The symbols used for the optic axes of the crystals and the vibration directions of the plane-polarized waves are the same as in Fig. 6.

9

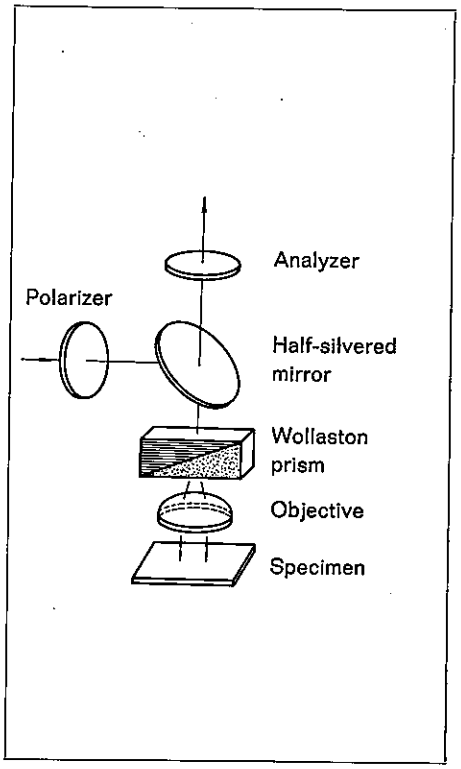

Fig. 9: Diagrammatic representation of a double-beam interference-contrast setup for reflected light using one Wollaston prism. For greater clarity, the lateral separation of the two beams striking the specimen has been exaggerated.

pass through the half-silvered mirror and, by means of an analyzer, are brought to vibrate in one plane. The interference-contrast image of the specimen is formed in the conventional manner in the intermediate image plane (not shown) and viewed through an eyepiece.

As regards the diagram in Fig. 9, it may be mentioned that the beam passing through the polarizer is inclined by 45° to the plane of the diagram. The polarizer should therefore be imagined as lying below the plane of the drawing. For this reason – and because of the perspective view – the vibration directions of the polarized components have not been indicated. In principle, however, conditions are similar to those shown in Figs. 7 and 8 for transmitted light.

4. The Nomarski double-beam interference-contrast microscope

The preceding remarks were primarily devoted to the design and operation of the birefringent components used to split and recombine the beams, while nothing was said about the effect of the specimen on the beams. This will be discussed together with the formation and interpretation of the interference-contrast image in the second paper to be published on this subject in this journal. We shall now examine what requirements have to be fulfilled by the image-forming optical system.

When discussing the double-beam interference-contrast microscope with two *Wollaston* prisms for transmitted light, we assumed that the lamp-side focal plane of the condenser and the eyepiece-side focal plane of the objective are located in the central planes of the *Wollaston* prisms (8, 15, 30, 31, 32). In addition, we assumed the interference planes of the *Wollaston* prisms, which coincide with their central planes (parallel to the upper and lower surfaces of the prism) to be exactly superimposed. The first of these requirements presents fundamental difficulties: with high-power objectives, the image-side focal plane lies in the objective, below the thread seat: a *Wollaston* prism can therefore not be located in that plane. This is equally applicable to transmitted-light and reflected-light objectives. But neither do transmitted-light condensers of high numerical aperture and correspondingly small focal length allow a *Wollaston* prism to be located in their front focal plane (i. e. on the side of the light source). As a result, differential interference-contrast microscopy with the aid of *Wollaston* prisms is limited to very low magnifications (30).

A very neat and technically feasible solution to these problems was the introduction of *Nomarski*'s modified *Wollaston* prism which in the following will be briefly called "*Nomarski* prism". This prism (Fig. 10) consists of two cemented components of a uniaxial, birefringent crystal, such as calcite or quartz. The optic axis of one of these prisms (the lower one in Fig. 10) is parallel to the wedge side, as in the *Wollaston* prism. The optic axis of the other prism, (the upper one in Fig. 10), however, is inclined at a certain angle to the upper bounding face. As a result, the interference plane is outside the compound prism (dashed line in Fig. 10). By suitable orientation of the *Nomarski* prism its interference plane can be made to lie in the eyepiece-side focal plane of the objective, although the *Nomarski* prism itself is located at a relatively long distance from the objective. This is of considerable importance for the design of a differential interference-contrast microscope: since the parfocal distance of the objectives, I. e. the distance between the object plane and the objective seating face, is given and constant, the *Nomarski* prism can likewise be mounted at a given distance from the objective, e. g. in an interference-contrast slide. Moreover, if the position of the eyepiece-side focal plane of the objectives used only slightly deviates axially from a certain mean position, a single *Nomarski* prism will suffice to recombine the beams with all available transmitted-light objectives. With the ZEISS interference-contrast equip-

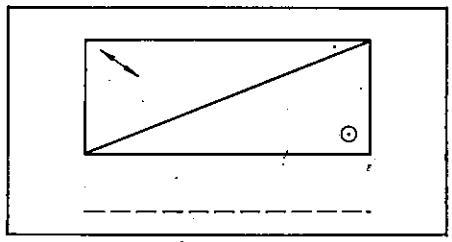

Fig. 10: Nomarski prism with direction of optic axes and position of interference plane indicated.

ment for transmitted light, one and the same *Nomarski* prism, i. e. the same interference-contrast slide[6], is used for objectives of 16 x, 40 x and 100 x. For this reason – and for other reasons which cannot be explained in detail here – this is called the principal prism, to distinguish it from the so-called secondary prisms accommodated in the substage condenser. In the ZEISS transmitted-light equipment, there are three secondary prisms which are contained in the achromatic-aplanatic condenser (type VZ) for interference contrast, phase contrast and bright field and designated as I, II and III. Like the different sizes of annular condenser diaphragms for phase contrast, the secondary prisms in the condenser are adapted to the numerical aperture (and the initial magnification) of the objectives to be used.

The terms "principal prism" and "secondary or compensating prism" are used in connection with an entirely different way of describing the differential interference-contrast microscope (8, 26, 30, 32). In the present paper, the design of the *Nomarski* differential interference-contrast microscope has for didactic reasons been described as that of a double-beam instrument. The aforementioned second approach is useful supplement and should therefore be briefly discussed: first, imagine all optical components such as the condenser (with secondary prism), specimen, objective and principal prism between the polarizer and the analyzer removed from the light path. The field of view will then be completely dark. If the principal prism, that is a birefringent component, is now inserted diagonally between polarizer and analyzer, the field will be partly illuminated; interference fringes will be visible parallel to the wedge sides of the component prisms; the fringes are black or colored, depending on whether monochromatic or polychromatic light is used for illumination (only the fringe or zero path difference will always be black). If the secondary prism is then moved into the light path together with the image-forming optics, the interference fringes of the secondary prism can be made to cancel out the fringes of the principal prism in the objective pupil, provided that the two prisms are suitably dimensioned and oriented: the field is once more completely dark. This corresponds to interference contrast explained above in connection with the interference microscope, which exists in the case of infinite fringe spacing.

While in the transmitted-light setup the principal and secondary prisms are separate, the principal prism of the reflected-light setup also acts as secondary prism. It is contained in the interference-contrast equipment into which the proper reflected-light objectives are screwed. The prisms are adapted to the numerical aperture of the objectives. – For further technical details and practical hints consult the literature listed overleaf (1, 2, 8, 24, 26, 29).

[6] The fact that the interference-contrast slide for the big STANDARD UNIVERSAL, PHOTOMICROSCOPE and ULTRAPHOT II is different from that of the STANDARD microscopes of the WL, RA and KL series is due to the different distance of the interference-contrast slides from the objectives (and other tube optics).

References:

[1] *Boelcke, C.:* STANDARD RA Routine and Research Microscope, Operating Instructions G 41-120, CARL ZEISS, Oberkochen.

[2] *Boelcke, C.:* Vertical Illumination on UNIVERSAL microscopes, PHOTOMICROSCOPE and ULTRAPHOT II. Operating Instructions G 41-655, CARL ZEISS, Oberkochen.

[3] *Born, M.,* and *E. Wolf:* Principles of Optics, third edition, Pergamon-Press Oxford-London-Edinburgh-New York-Paris-Frankfurt 1965.

[4] *Buchwald, E.:* Einführung in die Kristalloptik, 3rd ed., Sammlung Göschen, Leipzig 1937.

[5] *Flügge, J.:* Das Phasenkontrastverfahren nach Zernike und Erklärung des Interferenzkontrasts nach Nomarski. Lecture given at 1967 Course of Photomicrography held by CARL ZEISS, Oberkochen, at Göttingen.

[6] *Françon, M.:* Interférences, Diffraction et Polarisation, Handbuch der Physik XXIV (edited by S. Flügge), Springer-Verlag, Berlin-Göttingen-Heidelberg 1956.

[7] *Françon, M.:* Einführung in die neueren Methoden der Lichtmikroskopie, translated by L. Albert, Verlag G. Braun, Karlsruhe 1967.

[8] *Gabler, F.,* and *F. Herzog:* Eine neue Interferenzkontrasteinrichtung für Arbeiten im Durchlicht. Leaflet SD Interf. Kontr. DL D 8/66, C. Reichert, Optische Werke AG, Vienna.

[9] *Gahm, J.:* Polarized-light microscopy and double-beam interference microscopy by transmitted light, ZEISS Information 61 (1966), 89.

[10] *Gahm, J.:* Durchlicht-Interferenzeinrichtungen nach Jamin-Lebedeff, ZEISS-Mitteilungen 2 (1962), 389.

[11] *Hansen, G.:* Die Sichtbarkeit der Interferenzen beim Michelson und Twyman-Interferometer. ZEISS-Nachrichten, Vol. 4, No. 5 (1942), 109.

[12] *Hansen, G.,* and *W. Kinder:* Abhängigkeit des Kontrastes der Fizeau-Streifen im Michelson-Interferometer vom Durchmesser der Aperturblende. Optik 15 (1958), 560.

[13] *Illig, W.:* Oberflächenprüfung mit dem Interferenz-Mikroskop, Metalloberfläche 7 (1953), 97.

[14] *Jamin, M. J.:* Sur un réfracteur differentiel pour la lumière polarisée construit par Lutz, C. R. Acad. Sci. Paris 67 (1868), 814.

[15] *Jeglitsch, F.,* and *R. Mitsche:* Die Anwendung optischer Kontrastmethoden in der Metallographie, Radex-Rundschau, No. 3/4 (1967), 587.

[16] *Kinder, W.:* Ein Mikro-Interferometer nach W. Linnik, ZEISS-Nachrichten, Vol. 2 (1937), No. 3, p. 1.

[17] *Kinder, W.:* The Interference Flatness Tester and Interference Instruments for Surface Testing, ZEISS Information 58 (1965), 136.

[18] *Kohaut, A.:* Technische Interferenzmikroskopie, Hdb. d. Mikroskopie in der Technik (edited by H. Freund), Vol. I, Part 2, p. 555, Umschau-Verlag, Frankfurt a. Main 1960.

[19] *Krug, W., J. Rienitz,* and *G. Schulz:* Beiträge zur Interferenzmikroskopie, Berlin 1961.

[20] *Lebedeff, A. A.:* Interféromètre à polarisation et ses applications. Revue d'Optique 9 (1930), 385.

[21] *Michel, K.:* Die Grundzüge der Theorie des Mikroskops in elementarer Darstellung, 2nd ed., Vol. I of the "Physik und Technik" series, edited by F. Gössler, Wissenschaftliche Verlagsgesellschaft mbH, Stuttgart 1964.

[22] *Michel, K.:* Die Mikrophotographie, 3rd ed., Vol. X of the series "Die wissenschaftliche und angewandte Photographie", edited by J. Stüper, Springer-Verlag, Vienna-New York 1967.

[23] *Mütze, K., L. Foitzik, W. Krug,* and *G. Schreiber* (editors): ABC der Optik, Leipzig edition, Verlag Werner Dausien, Hanau/Main 1961.

[24] *Neupert, H.:* Nomarski interference-contrast equipment (CNRS licence), ZEISS Information 65 (1967), 96.

[25] Author not named: Transmitted-light interference equipment, leaflet 40-560/I, CARL ZEISS, Oberkochen.

[26] Author not named: Phase contrast and interference contrast, leaflet 41-210, CARL ZEISS, Oberkochen.

[27] Author not named: Wild Interference Attachments for Incident Light for the Wild M 20 Microscope. Leaflet M 1 421 e – VI. 67, Wild Heerbrugg Ltd., Switzerland.

[28] Author not named: Interference Microscope, leaflet 64-602/III, CARL ZEISS, Oberkochen.

[29] Author not named: Grand microscope auto-éclairant Nachet 300, Notice 1500, leaflet of Messrs. Nachet, Paris.

[30] *Nomarski, G.:* Microinterféromètre différentielle à ondes polarisées, J. Phys. Radium 16 (1955), 9.

[31] *Nomarski, G.,* and *Mme. A. R. Weill:* Sur l'observation des figures de croissance des cristaux par les méthodes interférentielles à deux ondes, Bull. Soc. franc. Minér. Crist. 77 (1954), 840.

[32] *Nomarski, G., and Mme. A. R. Weill:* Application à la métallographie des méthodes interférentielles à deux ondes polarisées, Rev. de Métallurgie 52 (1955), 121.

[33] *Piller, H.:* Durchlicht-Interferenzmikroskopie nach dem Jamin-Lebedeff-Prinzip, ZEISS-Mitteilungen 2 (1962), 309.

[34] *Pohl, R. W.:* Optik und Atomphysik, 10th ed., Springer-Verlag, Berlin - Göttingen - Heidelberg 1958.

[35] *Räntsch, K.:* Oberflächenprüfung durch Lichtinterferenz, Feinmechanik und Präzision 52 (1944), 75.

[36] *Räntsch, K.:* Optische Verfahren zur Oberflächenprüfung, ZEISS-Nachrichten, Vol. 5, 6 (1945), 189.

[37] *Räntsch, K.:* Grundsätzliches zur Interferenz-Mikroskopie, Werkstattechnik und Maschinenbau 42 (1952), 434.

[38] *Schulz, G.:* Zweistrahlinterferenzen: Über Interferenzprinzipien und den Ort der Interferenzerscheinung, Ann. Physik 13 (1953), 421.

[39] *Sievogt, H.:* Zur geometrischen Optik der Zweistrahl-Interferometer, Optik 11 (1954), 366.

[40] *Torge, R.:* The Interference Microscope, ZEISS Information 61 (1966), 100.

[41] *Uhlig, M.:* The ZEISS Interference Microscope in Practice, ZEISS Werkzeitschrift 30 (1958), p. 70.

II. Formation of the interference image

Part I of the general description of Nomarski differential interference-contrast microscopy dealt with the fundamentals and experimental designs of ZEISS interference-contrast equipment (12). This second part of the description will be devoted to the formation of the differential interference-contrast image (in the following called DIC image, following a suggestion by J. Gahm). For this purpose, the wavefronts of the Wollaston prism will be described first in Section 1. The background image, which depends on the differences of path length and amplitude of the interfering waves, is discussed in Section 2. The formation of the DIC image (Section 3) is explained with the aid of model objects. A detailed discussion of objects from the different fields of application of Nomarski DIC microscopy would be beyond the scope of this series of papers; it is therefore reserved for separate publication.

1. The wavefronts in the Wollaston prism

A wavefront is the line joining the points of identical phase within a wave packet (see, e. g., 1, 6, 11, 13, 14, 15, 23). The behavior of wavefronts in a Wollaston prism (18) will be explained with the aid of example a) of Fig. 1. In the lower crystal, a linearly polarized wave with the plane wavefront Σ is split into two plane-polarized components, viz. the ordinary wave and the extraordinary wave. Both waves have different refractive indices: with yellow sodium light of wavelength 589.3 mμ, the ordinary wave in a quartz crystal has a refractive index of n_o = 1.5442, the extraordinary wave one of n_{eo} = 1.5534. Consequently, the difference in refractive index is 0.0092, in other words, n_{eo} is almost 0.6 % larger than n_o. Since the propagation speed of the wave in the crystal is inversely proportional to the refractive index, it follows that the ordinary wave has a higher speed than the extraordinary wave[1]. As a result, the wavefront Σ_o is in advance of the wavefront Σ_{eo} in the lower prism.

So-called angular wave splitting occurs at the cemented surface, i. e. the ordinary and the extraordinary wave take different courses. The angle subtended by them is less than half a minute. In addition, the ordinary wave of the lower prism becomes the extraordinary wave in the upper prism, while the extraordinary wave of the lower prism becomes the ordinary wave in the upper prism (12, 15, 21). In case a) this means that in the upper prism the wavefront Σ_{eo} is in advance of the wavefront Σ_o because as Σ_o, Σ_{eo} has advanced beyond the second wave in the lower prism to such an extent that this advance is only slowly made up for in the upper prism. Since the angular splitting at the cemented surface is only very small, the geometrical paths of the two components in the central position of the Wollaston prism shown in the diagram are only slightly larger than in the lower half of the prism. Consequently, as the two waves emerge from the Wollaston prism, they have covered identical optical path lengths[2], i. e. both wavefronts leave the Wollaston prism simultaneously with zero path difference[2]. If after emerging from the Wollaston prism the two waves pass through air, the same refractive index applies to both of them, i. e. their speed is identical. As a result, the path difference between the two waves is maintained. In the special case a) it is zero.

If, for reasons that will be discussed later, a path difference is desired, this can be obtained by shifting the Wollaston prism perpendicular to the direction of the incident bundle of light. In case b), the advance of Σ_o over Σ_{eo} in the lower prism is such that it is compensated only partly in the upper half of the prism (wavefronts not shown): outside the Wollaston prism, Σ_{eo} advances in relation to Σ_o. The opposite case is shown in the example c).

In the experimental design of DIC equipment for transmitted light using two Wollaston prisms, a path difference can be introduced by shifting one of them because for the final DIC image it is of no importance whether the optical path difference is caused by the auxiliary prism in the condenser or whether it is introduced by means of the principal prism (12, 16, 17, 18, 20) located between objective and image. A displacement of the principal prism is given preference only for reasons of convenience. The most favorable conditions for this case follow from Fig. 1 if the diagram is imagined inverted. – If Nomarski prisms were utilized instead of Wollaston prisms, no basically new considerations would result with regard to the behavior of the wavefronts in the crystal (see 7, 18). The diagram thus obtained would merely be less clear than in the case of the Wollaston prisms discussed above.

2. The interference background image

In the following, the formation and interpretation of the *background* image in Nomarski DIC microscopy will be explained. By background image we understand the image of an object-free area in the specimen. With the ZEISS DIC equipment (and using white light for illumination of the object), this background can be made to appear black-and-white or gray or colored. This means that a multitude of different color phenomena may be encountered even if there is no microscopic object in the light path. These phenomena must not be attributed to a microscopic object, but considered as instrument characteristics, as equipment parameters[3]. A detailed explanation of the formation of the background image on one hand shows the multitude of optical staining possibilities. On the other hand it is intended to warn against possible sources of error in the interpretation of the interference image due to careless use of the equipment. – Before elaborating on the most essential characteristics of this equipment, a few concepts from the field of interference colors should be briefly reviewed.

---

[1] This holds generally for positively uniaxial crystals such as quartz. The opposite applies to negatively uniaxial crystals such as calcite (1, 21).

[2] Optical path length (2, 11, 13, 14, 15, 24): $\Delta = nd$, where n = refractive index, d = geometrical path. This is also called the path difference Γ, where Γ is preferably used for optical path differences, e. g. $\Delta_1 - \Delta_2$.

[3] In principle, these equipment parameters also apply to interference microscopes of other design, such as the Jamin-Lebedeff interference-contrast equipment made by ZEISS.

1

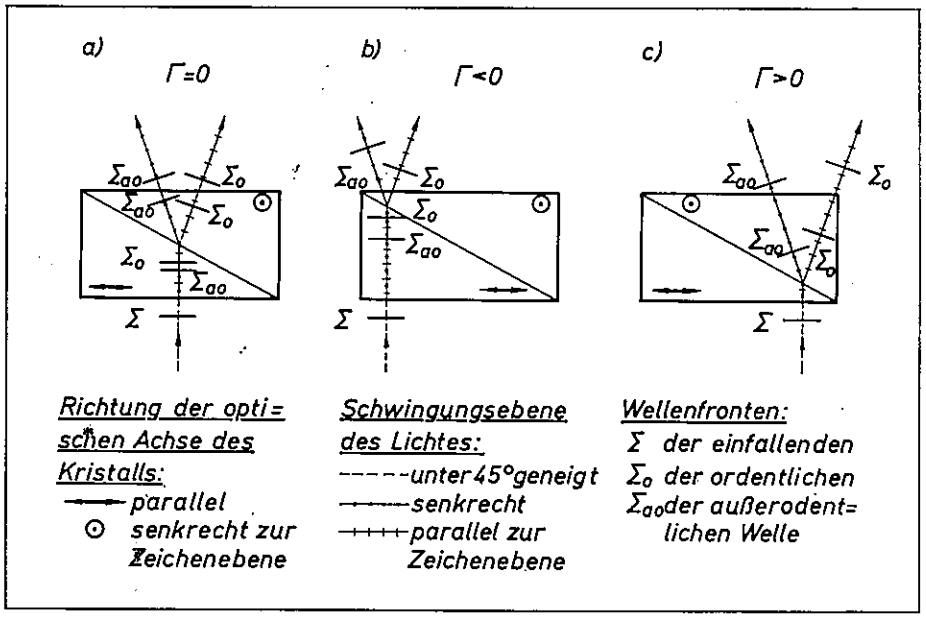

Fig. 1: Wavefronts in a Wollaston prism. For greater clarity, the angular wave splitting at the cemented surface and the distance between the wavefronts Σ_o and Σ_{eo} are exaggerated.

Richtung der optischen Achse des Kristalls = Direction of optic axis of crystal; parallel = parallel; senkrecht zur Zeichenebene = perpendicular to plane of diagram; Schwingungsebene des Lichtes = Vibration plane of light; unter 45° geneigt = inclined 45°; senkrecht = perpendicular; parallel zur Zeichenebene = parallel to plane of diagram; Wellenfronten = Wavefronts; der einfallenden Welle = of incident wave; der ordentlichen Welle = of ordinary wave; der außerordentlichen Welle = of extraordinary wave.

2

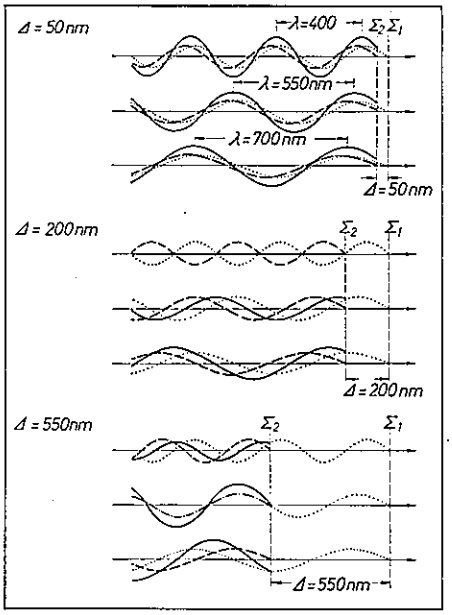

Fig. 2: Interference of white light. For simplification, only the colors blue, green and red are shown.

Fig. 2 shows schematically the conditions in the case of the superposition of two coherent wave packets of white light (11, 15, 22) with optical path differences Δ of 50, 200 and 550 mμ. For greater clarity, only three colors of the white light are shown, namely blue (wavelength λ = 400 mμ), green (λ = 550 mμ) and red (λ = 700 mμ). Making allowance for the sign, the interfering components (dotted and dashed curves) yield the solid curves as resulting waves. If the optical path difference between Σ_1 and Σ_2 is small, e. g. 50 mμ, as is shown in the upper part of the figure, then with all three colors the final curves have larger amplitudes than the individual curves: we then speak of constructive interference. The extreme is encountered if Δ = 0 or a whole multiple of the light wavelength. Thus in the lower part of the figure, the optical path difference of 550 mμ is equivalent to the wavelength of the green light. In this case the two components are "in phase", whereas, if Δ = 200 mμ, the two component beams of the blue light are of "opposite phase". They interfere destructively. This means that the white light is deprived of the blue component. The other final curves, in our example the green and red ones, will then mix uniformly in accordance with their intensity ratio[4] to form a so-called interference color. (To avoid misunderstandings, it should be pointed out here that this interference color is not identical with that of the DIC image.)

Since the intensity ratio of the different colors varies with optical path difference, every path difference is associated with a characteristic interference color. However, this applies only to path differences which do not exceed the coherence length (see 11).

In Fig. 2 it was tacitly assumed that the superimposed components (dotted and dashed curves) vibrate in one and the same plane. With interference microscopes this precondition, which is indispensable for the interference of two coherent waves, is not given from the start, but must be brought about with the aid of an analyzer. The same holds for the Nomarski DIC equipment: as is evident from Fig. 3a), an analyzer arranged between the principal prism and the eyepiece (18) intercepts the waves with the vectors of electrical field strength $\vec{e}_1$ and $\vec{e}_2$ and allows only the components $\vec{e}_{1A}$ or $\vec{e}_{2A}$ coinciding with the vibration direction of the analyzer A to pass (see 1, 6, 7, 12). The components $\vec{e}_{1P}$ or $\vec{e}_{2P}$, however, which together give $\vec{e}_P$, are perpendicular to the transmission direction of the analyzer and therefore have no effect on the final DIC image. In addition, the components parallel to the transmission direction of the analyzer shown in Fig. 3a) are of opposite, but identical magnitude so that they cancel out. Transferring these results to ZEISS DIC equipment, Fig. 3a) corresponds to zero path difference, i. e. the field of view is dark. The Michel-Lévy color chart (19) reveals that zero path difference is equivalent to the interference color black.

If there is a path difference between the two waves emerging from the principal prism, then $\vec{e}_1$ and $\vec{e}_2$ differ in length (Fig. 3b). Consequently, the length of the components $\vec{e}_{1A}$ and $\vec{e}_{2A}$ also differs. In the DIC image, the resultant of these two vectors, namely $\vec{e}_A$, becomes effective. (The vector $\vec{e}_P$ resulting from $\vec{e}_{1P}$ and $\vec{e}_{2P}$ is perpendicular to the transmission direction of the analyzer and thus does not contribute to the DIC image.) – If the path difference is 50 mμ, e. g. as in Fig. 2, top, the DIC image will assume a hue between iron and lavender gray, as is also evident from the Michel-Lévy color chart (6). A gray blue to gray or deep red hue in the DIC image corresponds to a path difference of 200 or 500 mμ, respectively (see Fig. 2).

If polarizer and analyzer are not accurately crossed (Figs. 3c and d), the DIC image will be affected in a different way. While $\vec{e}_1$ and $\vec{e}_2$ are of identical length in Fig. 3c) (which corresponds to zero path difference), their components in the transmission direction of the analyzer, $\vec{e}_{1A}$ and $\vec{e}_{2A}$, are of dif-

[4] Due to the difference in wavelength the final curves of the different colors cannot interfere. The intensity ratio is therefore decisive for the resultant interference color.

ferent magnitude. The resultant $\vec{e}_A$ therefore differs from zero (in spite of zero path difference). It lights the image background. The vector $\vec{e}_A$ resulting from $\vec{e}_{1A}$ and $\vec{e}_{2A}$ is perpendicular to A and therefore cannot affect the interference image.

If, in addition, there is a path difference between the components 1 and 2, $\vec{e}_1$, $\vec{e}_2$ and thus $\vec{e}_{1A}$, $\vec{e}_{2A}$ will also differ in length (Fig. 3d). The resultant $\vec{e}_A$ strikes the DIC image in a different way than is the case in Fig. 3b). To avoid unnecessary difficulties in the interpretation of the DIC image, it is therefore advisable to work with crossed polarizer and analyzer.

3. The DIC image

In interference microscopes, the "object structure" seen in the microscopic image is the optical expression of very different physical magnitudes of the microscopic object. With the Nomarski DIC equipment described in this paper, the interference image of an isotropic phase object depends a) on the magnitude of the angular or lateral wave splitting and b) on the path difference between the two components (see also 6, 7, 11, 23). The path difference caused by a *transparent* object is given by the product of the refractive index and geometrical thickness of the object. As is shown in Section 2, an additional path difference can be superimposed by means of the principal prism.

The path difference caused by an *opaque* object depends on the geometrical profile of the object and the phase retardation resulting from reflection of the waves from the opaque object. In this case also an additional path difference can be introduced with the aid of the Wollaston (or Nomarski) prism which in the reflected-light equipment is traversed twice and therefore acts both as an auxiliary and a principal prism (12, 16, 17, 18, 20).

Fig. 4 shows on the left a diagram of a DIC unit for transmitted light using two Wollaston prisms. A body of rectangular cross section is represented as an isotropic, i. e. nonbirefringent object (specimen slide, mounting medium and cover glass are not shown). The condition of the wavefronts at the points a to d in the light path is illustrated in the right-hand part of Fig. 4. The intensity distribution of the DIC image formed in the intermediate image plane, marked e in the diagram, is also discussed. Let the refractive index of the object be smaller than that of the mounting medium: the portions of the wavefronts passing through the object are then accelerated, i. e. they are advanced in relation to the portions of the wavefronts not affected by the object. The resulting wavefront deformation is all the larger, the greater the thickness and smaller the refractive index of the object.

3

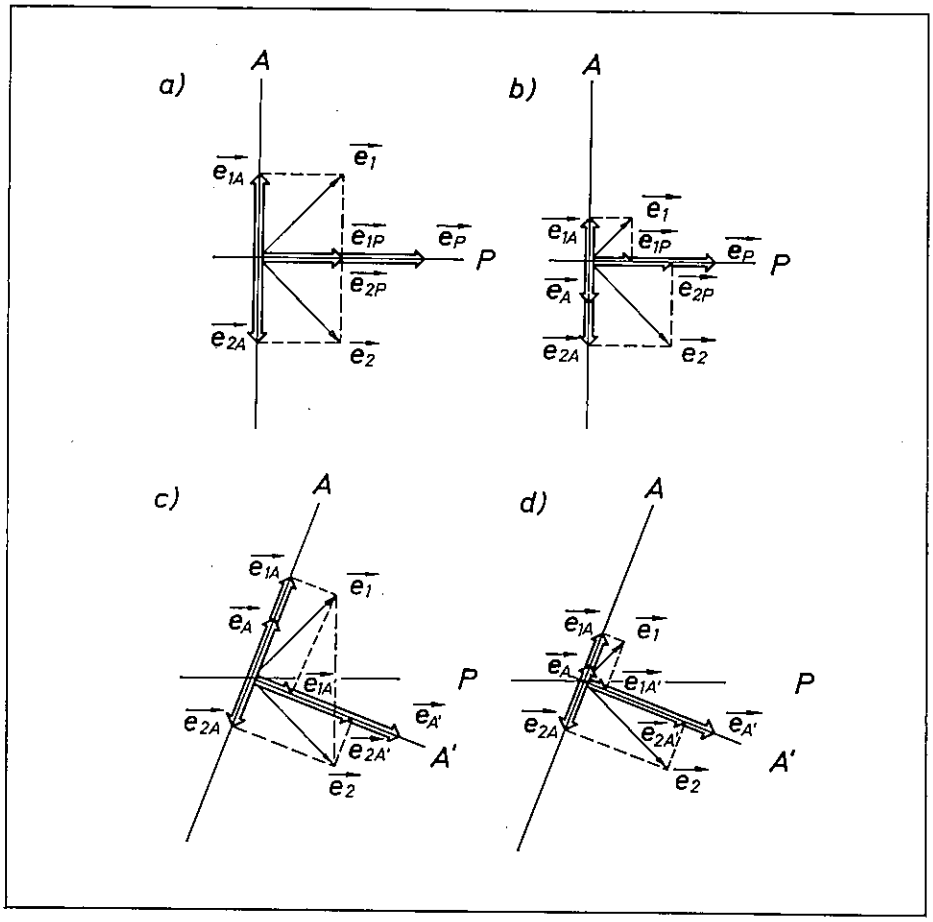

4

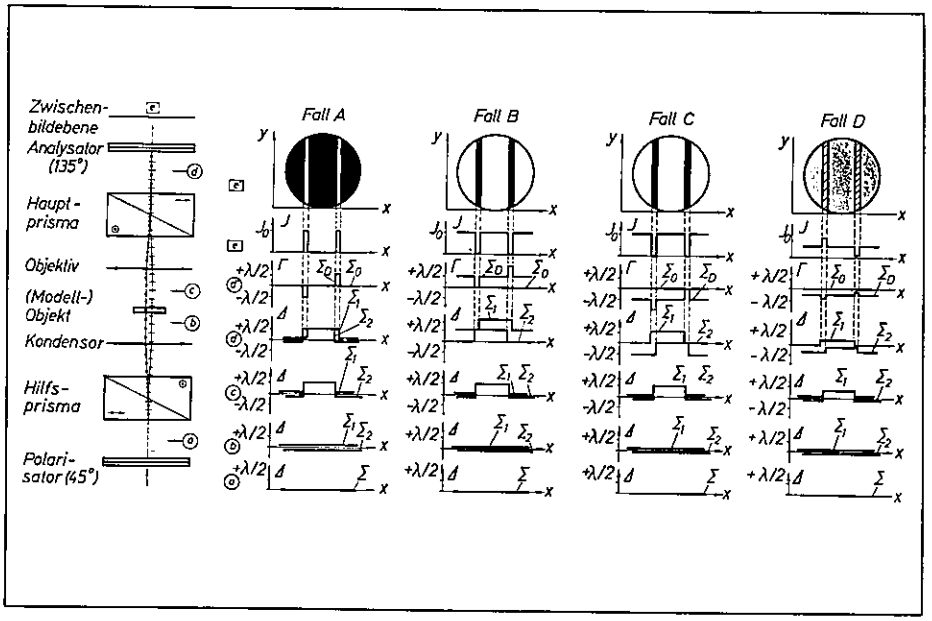

Fig. 3: The effect of the analyzer in ZEISS DIC equipment. P = transmission direction of polarizer, A = transmission direction of analyzer, A′ = direction perpendicular to A, $\vec{e}$ = vector of electrical field strength, index 1 or 2 = waves emerging from principal prisms with mutually perpendicular vibration planes. a) crossed P and A. $\Gamma = 0$ between waves 1 and 2; b) same as a), but $\Gamma = 0$; c) P and A not rigorously crossed. $\Gamma = 0$; d) same as c), but $\Gamma = 0$.

Fig. 4: Wavefronts at different points in the light path and intensity distribution in the intermediate image plane of a DIC unit in accordance wih the diagram in the lefthand portion of the illustration. Cases A to D are distinguished by the path differences between the wavefronts Σ_1 and Σ_2.
Zwischenbildebene = Intermediate image plane; Analysator (135°) = Analyzer (135°); Hauptprisma = Principal prism; Objektiv = Objective; (Modell-) Objekt = (Model-) object; Kondensor = Condenser; Hilfsprisma = Auxiliary prism; Polarisator (45°) = Polarizer (45°); Fall = Case.

5

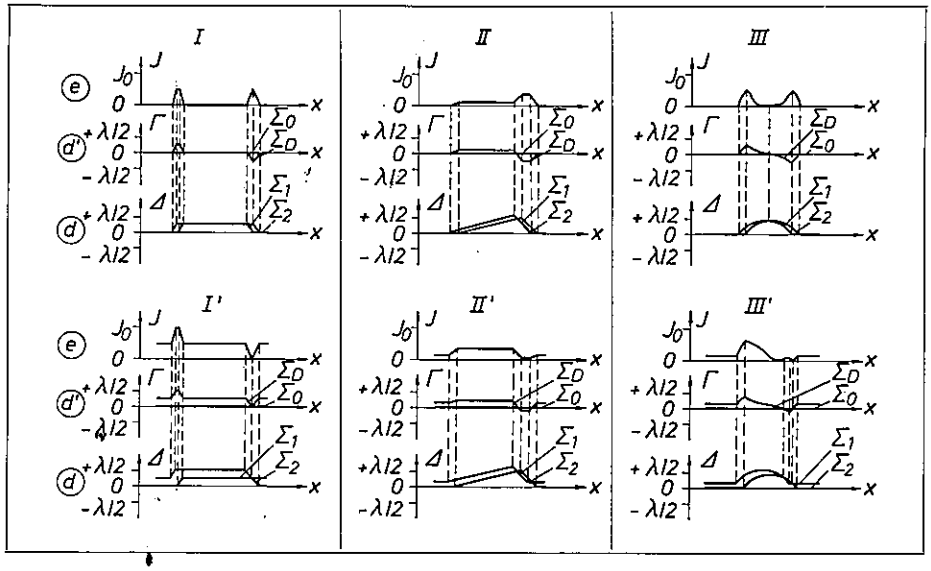

6

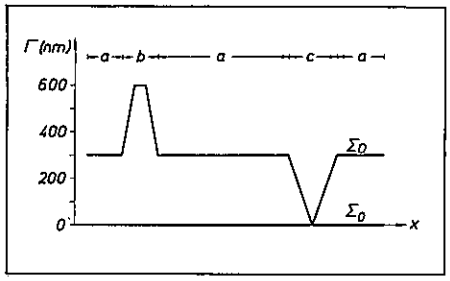

7

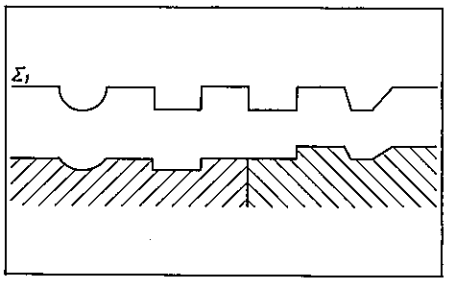

Fig. 5: Deformed wavefronts with the resulting intensity distribution in the x-direction of the DIC image. Path differences in background = zero (I, II, III) or not zero (I', II', III').

Fig. 6: Color contrast in DIC image.

Fig. 7: Deformation of a plane wavefront by an opaque object with two different phases.

In the cases A to C the path difference is assumed to be $+\lambda/2$, and in case D $+\lambda/8$ (diagrams c).

In case A it is assumed that no additional path difference is introduced between Σ_1 and Σ_2 by the principal prism. The function of the principal prism is thus essentially to cancel the angular wave splitting produced by the auxiliary prism. In the process, however, a lateral displacement of the wavefront deformations occurs (d), so that path differences are, after all, introduced between Σ_1 and Σ_2. But the path differences thus caused can only occur at points of the wavefronts where the object has already introduced a change of path difference Γ by the x-coordinate. For the DIC image only the difference of optical paths between Σ_1 and Σ_2 is of importance. Making due allowance for the sign, this is obtained by subtracting the wave Σ_2 from Σ_1[5]. The result is shown in diagram d'. If – following a suggestion by Nomarski (16, 17, 18) – this difference or the differential wave Σ_D is assumed to be an undisturbed reference wave, supplemented by a second, plane wave Σ_0, then the representation in d' is equivalent to d. It is, however, considerably clearer, an advantage that is felt above all with complicated deformed wavefronts.

If *monochromatic* light is used, the simplified relationship $I = I_0 \sin^2(\phi/2)$ holds for the intensity distribution of the DIC image, where I_0 is the maximum intensity in the image and ϕ the phase angle. An angle $\phi = 360°$ corresponds to a path difference $\Gamma = \lambda$. For $\Gamma = -\lambda/2$ corresponding to $\phi = -180°$, $\sin(-180°/2) = -\sin 90° = -1$ and $I = I_0 (-1)^2 = I_0$. The same value is obtained for $\Gamma = +\lambda/2$. For $\Gamma = 0$, I also becomes zero. Thus all values required to indicate the intensity distribution in the x-direction in the diagram e are known. The diagram e' gives an idea of the intensity distribution in the x and y-directions, as in practice the DIC image is seen as a circular disk in the intermediate image plane. In the example, two bright bands can be seen against a completely dark background. These bands indicate that in the corresponding specimen area the optical thickness noticeably differs in the x and/or y-directions from that at directly adjacent points.

Only this causes the deformation of the originally plane wavefronts, and only those points in which Γ varies in the x (and/or y) direction become visible in the DIC image. In the present case, the fringe *spacing* is at the same time a measure of the width of the phase object. The fringe *width* depends on the lateral wave displacement in the equipment; it is chosen so that it is smaller or, at best, identical to the microscopic resolving power. In addition, the fringe width depends on the change of path difference in the x and y-directions (on the gradient of Γ) and thus on the object or the specimen (see examples in Fig. 5).

The DIC image e' in case B of Fig. 4 shows two black fringes on a bright background. Consequently, case B is complementary to A. The inversion of the brightness distribution is brought about by the path difference $+\lambda/2$ between Σ_1 and Σ_2 (diagram d). – In case C (diagram d), Σ_1 lags behind Σ_2 by $\lambda/2$. The same intensity distribution (e') is obtained as in case B. With the principal prism in opposite positions, i. e. symmetrical to the zero position, both these cases can be realized.

In case D, the path difference caused by the object is assumed to be $\lambda/8$ and the path difference introduced by the principal prism $\lambda/4$ (d), contrary to A, B and C. Computation of the intensity distribution yields a different brightness of the two fringes. The impression is that of one-sided oblique illumination of the object (7, 20) with the well-known three-dimensional character[6]. (See also Figs. 48, 81, 443 in Michel [14]).

Fig 5 contains further examples of the formation of DIC images of different isotropic phase objects. Here only those diagrams are included which are essential to the understanding of the problem. The diagrams that have been omitted can easily be added in accordance with the example shown in Fig. 4. If *white* light is used instead of monochromatic light, the contrast of the object is increased by interference colors.

---

[5] This purely formal transformation is carried out exclusively for reasons of convenience and has nothing to do with the subtraction or addition of interfering waves required in interference microscopy. Before reaching the analyzer, Σ_1 and Σ_2 cannot interfere for the simple reason that their vibration directions are mutually perpendicular.

[6] DIC images of a phase object similar to the model under discussion are found elsewhere (20). It should be noted that the photomicrographs published there show two parallel furrows in the evaporated film of a specimen slide so that a total of four edges can be seen; the model object in Fig. 4 can, of course, produce only two edges. – Case A is, in general, comparable to Fig. 36 a (in 20), case C (and case B) to 36 c, and D corresponds to 36 b.

This will be explained with the aid of a wavefront (see also [6]), which in a similar form was used already in Fig. 5 (l' d'), to demonstrate the process of image formation by monochromatic light. This is why optical wavelengths and path differences are indicated on the ordinate in multiples of half the wavelength of the light used. This is, of course, inappropriate in the case of white light.

In the ranges "a" of Fig. 6, Γ is 300 mμ, which according to the Michel-Lévy color chart (19) corresponds to yellow of the first order. In the range b, Γ rises from 300 to 600 mμ, colors ranging from first-order yellow to second-order blue being traversed. However, the intermediate interference colors are less pronounced, since they are relatively crowded due to the considerable variation of Γ. The same applies to the other end in the b range. The color of the plateau (roughly indigo) can, however, be recognized more clearly. In the c range, the variation of Γ with x is not as abrupt as before. The colors are therefore easier to recognize, viz. yellow and first-order white at the upper edges of the furrows, followed by various gray hues which finally become black at $\Gamma = 0$.

The remarks on the formation of the DIC image with transmitted light also hold for reflected light. Characteristic differences exist only in two points. Firstly, a single Wollaston or Nomarski prism represents the auxiliary and principal prisms in the reflected-light equipment. However, such an arrangement can be formally transformed into a transmitted-light setup, as was explained elsewhere (12). Secondly, there is an essential difference in the causes of the wavefronts deformed by the object. In the case of isotropic transparent objects, the local product of refractive index and geometrical thickness of the object determines the form and extent of the wavefront deformation. With opaque objects, the surface relief and thus the geometrical path as well as the phase retardation due to reflection of the wave from the object (21) determine the shape and magnitude of the wavefront deformation (6, 11, 23). This is illustrated by Fig. 7. Let the opaque object consist of two phases (hatched), which impart a different amount of retardation to the reflected waves. A plane wavefront reflected by the object is transformed into the wavefront Σ_1. The rectangular deformations may at the same time serve as an example of ambiguous image formation (see also Fig. 4, B, C; for further examples, see publications 6, 11, 18, 23). Special cases like these are possible in principle if the final image is, among other things, the result of two different magnitudes, such as the thickness and refractive index of the object. An unambiguous interpretation is then possible only on the basis of additional information or measurement using one of these two magnitudes.

References:

[1] *Buchwald, E.:* Einführung in die Kristalloptik, 3rd edition, Sammlung Göschen, Leipzig 1937.

[2] *Flügge, J.:* Leitfaden der geometrischen Optik und des Optikrechnens, Vandenhoeck & Ruprecht, Göttingen 1956.

[3] *Flügge, J.:* Das Phasenkontrastverfahren nach Zernike und Erklärung des Interferenzkontrasts nach Nomarski, lecture given in 1967.

[4] *Françon, M.:* Rev. d'Opt. **31** (1952) 65.

[5] *Françon, M.:* Interférences, Diffraction et Polarisation, Handbuch der Physik XXIV (edited by S. Flügge), Springer-Verlag Berlin-Göttingen-Heidelberg 1956.

[6] *Françon, M.:* Einführung in die neueren Methoden der Lichtmikroskopie, translated by L. Albert, Verlag G. Braun, Karlsruhe 1967.

[7] *Gabler, F.* and *F. Herzog:* Leaflet SD, Interference Contrast, DL D 8/66 by Messrs. C. Reichert, Vienna.

[8] *Gahm, J.:* ZEISS-Information No. 46, pp. 118 – 127.

[9] *Herzog, F.:* Industrie-Anzeiger No. 60 of July 27, 1962.

[10] *Jeglitsch, F.* and *R. Mitsche:* Die Anwendung optischer Kontrastmethoden in der Metallographie, Radex-Rundschau, No. 3/4 (1967), 587 – 596.

[11] *Krug, W., J. Rienitz* and *G. Schultz:* Beiträge zur Interferenzmikroskopie, Akademie-Verlag, Berlin 1961.

[12] *Lang, W.:* Zeiss-Information No. 70 (1968) 113.

[13] *Michel, K.:* Die Grundzüge der Theorie des Mikroskops in elementarer Darstellung. 2nd edition. Wissenschaftliche Verlagsgesellschaft mbH, Stuttgart 1964.

[14] *Michel, K.:* Die Mikrophotographie, 3rd edition, Springer-Verlag, Vienna – New York 1967.

[15] *Mütze, K., L. Foitzik, W. Krug* and *G. Schreiber* (editors): ABC der Optik, Hanau/Main 1961.

[16] *Nomarski, G.:* J. Phys. Radium **16** (1955) 9.

[17] *Nomarski, G.* and *Mme. A. R. Weill:* Bull. Soc. Franc. Minér. crist. **77** (1954) 840.

[18] *Nomarski, G.* and *Mme. A. R. Weill:* Rev. de Métallurgie **52** (1955) 121.

[19] Author not named: Supplement to leaflet S 40-554 of Messrs. Carl Zeiss.

[20] Author not named: Leaflet 41-210 of Messrs. Carl Zeiss.

[21] *Pohl, R. W.:* Optik und Atomphysik, 10th edition, Springer-Verlag, Berlin-Göttingen-Heidelberg 1958.

[22] *Räntsch, K.:* Feinmechanik und Präzision **52** (1944) 75.

[23] *Rienitz, J.:* Mikroskopie **22** (1967) 169.

[24] *Zimmer, H. G.:* Geometrische Optik, Springer-Verlag, Berlin-Heidelberg-New York 1967.

III. Comparison with phase contrast

Part I of the general description explained the fundamentals and the experimental setup for Nomarski differential interference-contrast (DIC) microscopy (11). Part II dealt with the formation of the DIC image (12). The present part III is devoted to a comparison between the characteristics of DIC equipment and those of phase-contrast (PC) equipment. This comparison is limited to transmitted-light instrumentation. A comparison with reflected-light equipment will be published elsewhere. A final section, part IV, will discuss the uses of Nomarski DIC microscopy.

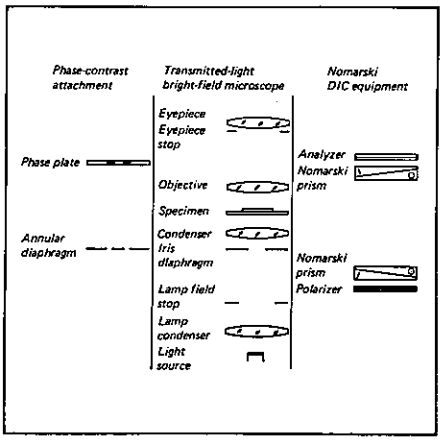

Fig. 1: Diagram illustrating the conversion of a ZEISS transmitted-light bright-field microscope for Zernike phase contrast and Nomarski differential interference contrast.

1. Experimental setup

The great majority of biological specimens are so-called phase objects. Pure phase objects (as compared to amplitude objects) do not affect the amplitude of the waves transmitted by the object. Apart from the diffraction of the light by object details, phase objects modify the path difference between the waves passing through the object field and those traversing the surrounding field. However, the human eye acting as a detector during visual observation of the microscopic bright-field image is unable to recognize these path differences. To make them visible, the light path has to be suitably modified.

The light path of ZEISS transmitted-light bright-field microscopes can be modified by the user, due to the availability of suitable accessories. (The same applies to ZEISS reflected-light microscopes.) To convert a bright-field microscope for phase-contrast observation (Fig. 1), it is necessary to exchange the condenser iris for an annular diaphragm and to mount a phase plate, optically conjugated to the condenser annulus, in the exit pupil of the objective. Since the pupil of microscope objectives, above all of high-aperture and high-power types, is in the interior of the optical system, special phase-contrast objectives are made for phase work, which, following a suggestion by K. Michel, have the phase plate in a cement layer between lens elements. (The history of the phase-contrast technique is discussed in [9, 10]).

To convert a bright-field microscope for interference microscopy (Fig. 1), it is only necessary to add a polarizer and a Nomarski prism below the front focal plane of the condenser and a second Nomarski prism as well as a second polarizer (as analyzer) above the objective (see 17).

2. Characteristics of ZEISS PC and DIC equipment

A comprehensive discussion of the differences between phase-contrast and interference-contrast accessories is beyond the scope of this series of papers. The following explanations will therefore be limited to the description of a few characteristic properties of these two optical staining methods.

2.1 Azimuth effect

The specific components required for phase contrast are rotation-symmetric. As a result, the PC image of a phase object is independent of the angular, i. e. azimuth orientation of the object in relation to the PC system. By contrast, the Nomarski DIC system is not rotationally symmetric but has a pronounced preferential direction (1, 8, 23). This direction is given by the design of the Nomarski prism and its fixed angular orientation relative to the polarizer and analyzer. Owing to the asymmetry of the Nomarski prism in relation to the optical axis of the microscope, the DIC effect is produced in the direction of the prism edges, but not perpendicular to them, because the differential retardation of waves is effective only in the direction of the prism edges (1, 11, 12, 19, 20, 21). The effect of this phenomenon is illustrated in Fig. 2.

However, this disadvantage of DIC equipment is rarely found disturbing. It is particularly pronounced in linear phase objects extending in the direction of shear.

If a rotary specimen stage is used, the linear object can always be oriented so that the detail of interest is imaged with optimum differential interference contrast. Non-linear objects hardly show this azimuth effect (see Figs. 4 to 7).

2.2 Halo effect

Haloes in the image of object edges are typical of phase contrast. In positive phase contrast[1], the edge of an object of higher refractive index than its surroundings has a bright fringe on the outside and a dark one on the inside (halo effect). The opposite is the case when an object of lower refractive index than its surroundings is viewed in positive phase contrast. Brief mention should here be made of the causes of the halo phenomenon[2]. Objects of a pronounced phase nature can be recognized in a bright-field microscope only with difficulty – if at all – since they hardly attenuate the light incident on them. However, a small portion of the incident radiation is deflected out of its original direction; it is diffracted by the phase object. By comparison with the non-diffracted light, the diffracted rays are shifted in phase by 90°. In Zernike phase contrast (28, 29)

[1] All ZEISS phase-contrast accessories are designed for positive phase contrast. As a result, objects whose optical thickness is greater than that of the surrounding field appear dark against a bright background.

[2] For references, see, for example, 2, 4, 5, 6, 7, 13, 14, 15, 16, 22, 26.

a) the direct light is also shifted in phase by 90°,

b) the intensity of the direct light is reduced until it is comparable to that of the diffracted light,

c) the diffracted light and the direct light of reduced intensity and shifted phase are superimposed on each other for interference.

The ZEISS phase-contrast equipment satisfies all these conditions with the aid of an absorbing annular phase plate in the front focal plane of the objective.

The phase plate accelerates the light by 90° (positive phase contrast). In order to reduce the effect of the phase plate on the direct light as much as possible, a hollow cone of ligth produced by the annular condenser diaphragm is used for illumination. In spite of this precaution, a certain part of the diffracted light will also pass through the phase plate because whenever radiation is transmitted by the specimen, every point of the phase object becomes a wave center from which the diffracted light is deflected in certain directions. The smaller the object detail, the larger is the angle of diffraction. If the phase object is of appreciable extension and differentiated structure (which is practically always the case with biological objects), the diffracted light will also pass through the phase plate (shaded beam in Fig. 3 [see 24]). An additional path difference of 90° (undesirable but unavoidable) is imparted to this light. It interferes constructively with the direct light in the intermediate image plane, i. e. its intensity is increased (bright fringe). On the one hand, the intensity and extent of the halo effect are equipment factors determined by the amount to which the undiffracted light is absorbed and shifted in phase by the phase plate. On the other hand, the halo effect varies with the size of the object (23), a phenomenon that will be discussed in greater detail in the next paragraph. In addition, however, the halo effect is also a function of the difference in refractive index between the object and its surrounding field (8, 23), as is evident from Fig. 7.

On the whole, the halo effect is thus partly due to equipment conditions. While it can be reduced to a certain extent by suitable design of the phase-contrast accessories, it cannot be eliminated altogether.

A one-sided lightening of object edges similar to the halo effect is sometimes observed in differential interference contrast also. However, this phenomenon is due to entirely different causes which were explained in Part II in connection with the description of DIC image formation (12).

[3] Figs. 4 and 7 courtesy of Prof. Dr. P. Stoll and Dr. H. Gundlach.

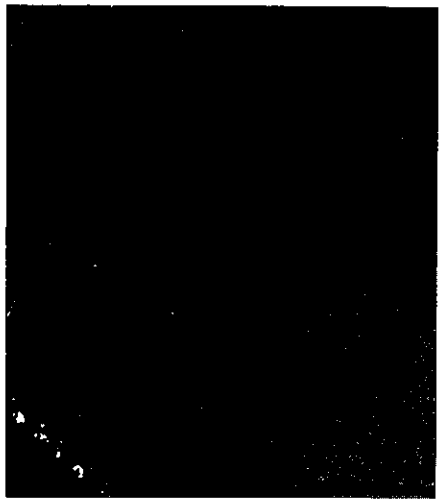

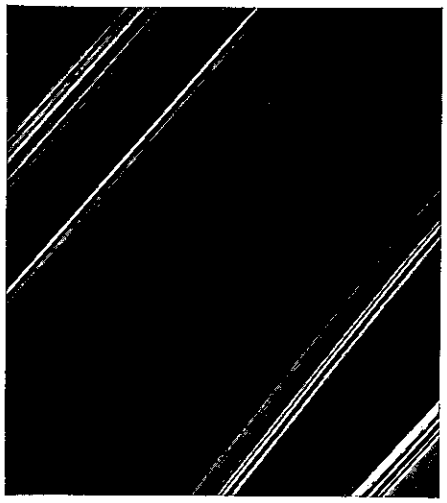

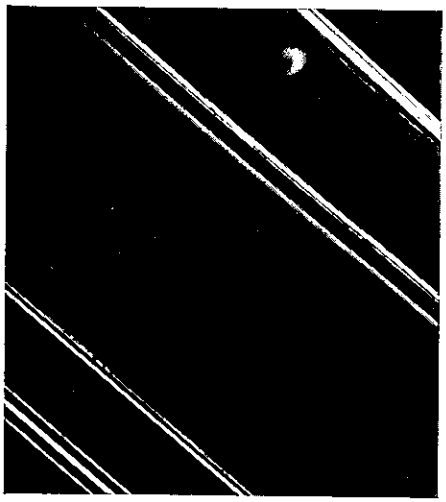

Fig.: 2 Optical staining of oriented linear phase objects (scratches in specimen slide).
Top: DIC image. The grooves extend in the direction of shear. Only details which exhibit very pronounced changes of optical thickness in a minimum of space stand out against the background.
Center: DIC image. Object turned through 90° and thus aligned for optimum contrast.
Bottom: PC image. Alignment of the object has no effect on contrast. Photomicroscope II, 40x N. A. 0.65 Planachromat and 40x N. A. 0.75 Ph-2 Neofluar, total magnification approx. 530x.

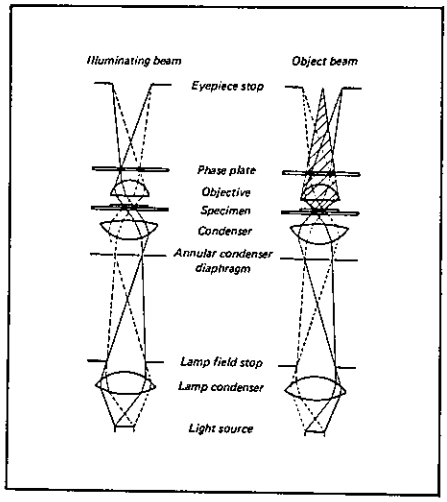

Fig. 3: Optical diagram of transmitted-light microscope with phase-contrast equipment.

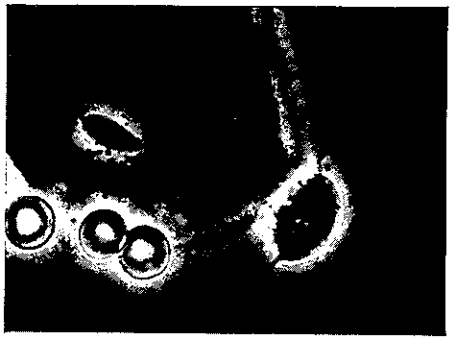

Fig. 4: The halo effect in PC microscopy with phase objects of "medium" size. The illustration[3] shows a gynecological smear in a saline solution: living trichomonad beside an epithelial cell and erythrocytes. Top: phase contrast, bottom: differential interference contrast. Photomicroscope. 40x N. A. 0.75 Neofluar and 40x N. A. 0.65 Planachromat. Total magnification approx. 530x.

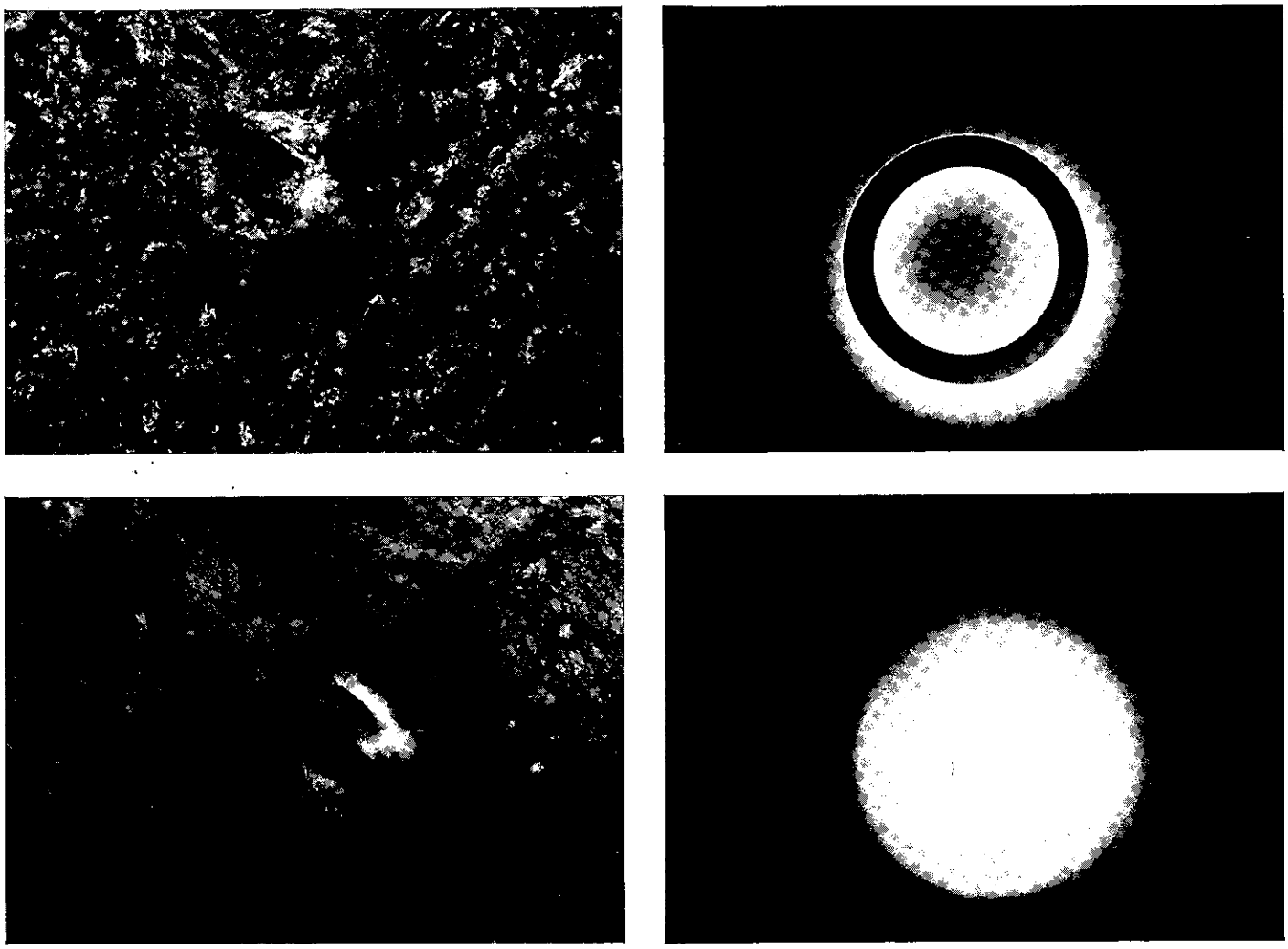

Fig. 5: This specimen (polished bone, tetracycline-labeled for fluorescence microscopy by reflected light) is unsuitable for observation by transmitted light because it is too thick and does not lie flat on the specimen slide. Exact reproduction of the contrast-generating PC or DIC elements is not possible under these conditions.
Top left: PC image. Right: pupil. Bottom left: DIC image. Right: pupil. Photomicroscope. 16x N. A. 0.35 Planachromat and 16x N. A. 0.40 Ph-2 Neofluar; Optovar 1.25x. Total magnification approx. 170x.

2.3 Object size and differences of refractive index

There is a direct connection between the halo effect in phase-contrast microscopy and the limited range of object sizes suitable for optimum reproduction in phase contrast (1, 7, 23). For the reasons mentioned under 2.2, the phase structure of phase objects of „medium" size is not reproduced with high fidelity because the phase plate of the Ph-objective has an undesirable effect on the light they diffract. Which object size should in practice be considered as "medium" depends on one hand on the size of the annular condenser diaphragm (with conjugate phase plate) and on the other on the magnification of the PC system used. A phase object, for example, which reveals the halo effect when observed with type Ph-2 phase accessories, should be considered as of "medium" size. If the same object is examined with a phase-contrast objective of higher power (Ph-3 with appropriate annular condenser diaphragm), it may then be considered as large. It is thus quite possible that one and the same object may show haloes under medium magnification but be free from haloes at high powers.

However, it should be noted that object size alone (for a given PC system) is not enough to explain the halo effect. Another factor to be taken into account is the difference in refractive index between the object and the mounting medium. The greater this difference, the more pronounced the halo effect (8, 14). It is therefore quite possible that not only objects of medium size but also small objects, for instance, exhibit a pronounced halo effect (see Fig. 7). By adapting the refractive index of the mounting medium to that of the object, these haloes can be drastically reduced.

Contrary to phase work, DIC microscopy is not characterized by such a pronounced dependence of image quality on the size of phase objects. DIC microscopy can be equally well applied to small, medium and large microscopic phase objects without any impairment of image quality (1, 7, 23). However, this applies only to interference microscopes using the principle of differential shearing, i. e. in which the lateral shift of wave fronts (12) is smaller or equivalent to the microscope's resolution (7). In the case of interference microscopes based on total splitting – e. g. the ZEISS Jamin-Lebedeff transmitted-light interference attachment – the admissible object size must be smaller than the separation between the measuring beam and the reference beam (11) to give satisfactory results.

Another advantage of Nomarski DIC microscopy comes as a welcome supplement to PC microscopy: pronounced differences of refractive index between the object and the mounting medium, which give rise to disturbing haloes in the phase-contrast image, are highly desirable for DIC work. They give images of excellent contrast and allow minute details to be recognized (e. g. Fig. 7, lower part of picture) which in phase contrast are hidden by bright fringes around the object.

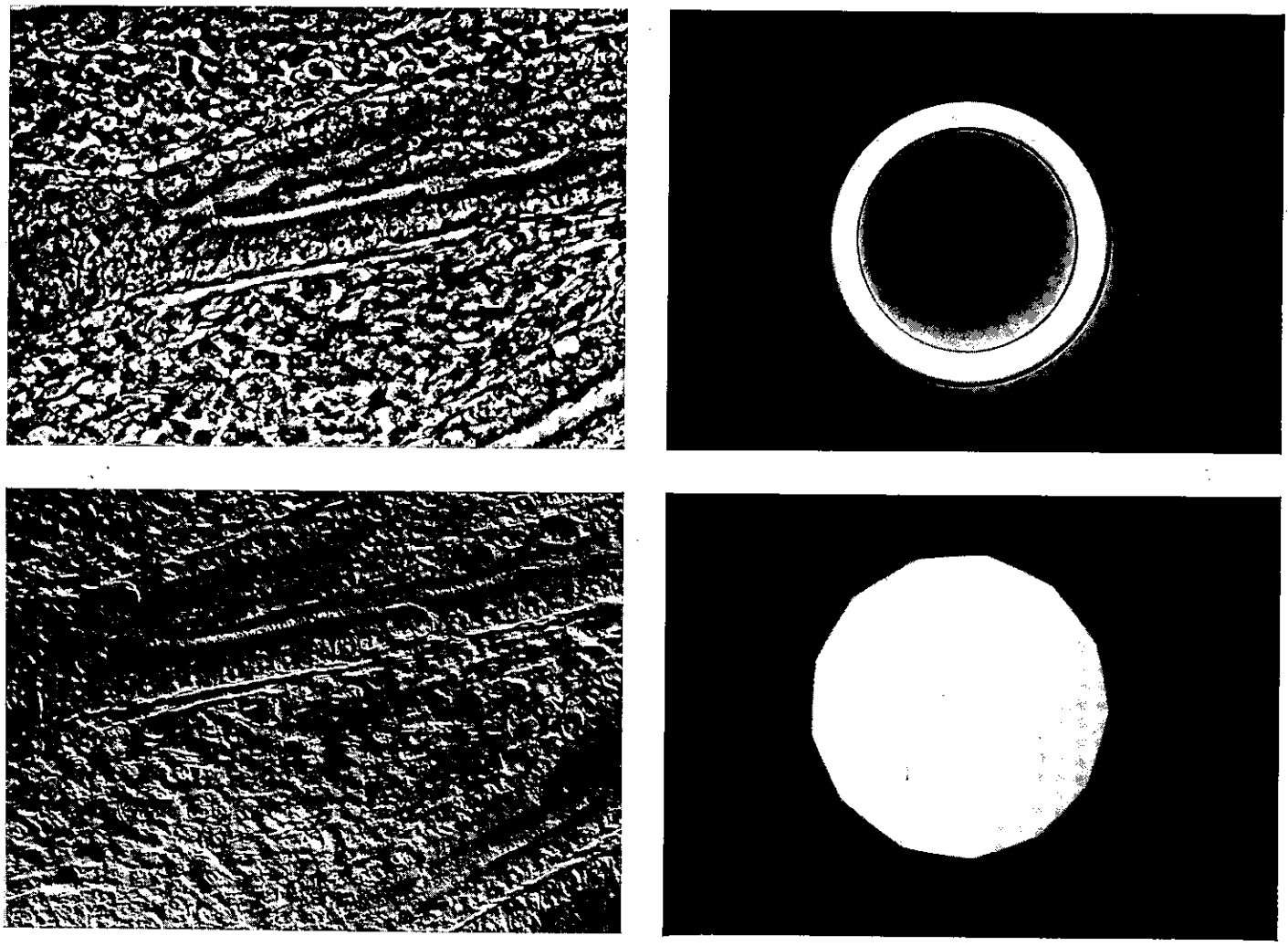

Fig. 6: Specimen suitable for examination by transmitted light (rat's tongue, unstained). Top left: PC image. Right: pupil. Bottom left: DIC image. Right: pupil. Photomicroscope, 16x N. A. 0.35 Planachromat and 16x N. A. 0.40 Ph-2 Neofluar; Optovar 1.25x. Total magnification approx. 170x.

2.4 Optical thickness of the object

The difference between the optical thickness (product of refractive index and geometrical path length) of the object field and the surrounding field determines the optical path difference Γ between object wave and field wave. The phase angle φ in degrees can be computed, as is known, from the relationship $\varphi = \Gamma\ 360°/\lambda$ where λ is the wavelength of the monochromatic light used. Let the expression $K = (E_{max} - E_{min})/E_{max}$ be the contrast, with E_{max} and E_{min} the maximum and minimum radiant intensity, respectively, of the microscopic image. Plotting contrast against phase angle, we obtain information on the optimum range in which a microscopic technique should be used. According to Michel (14, p. 110), a phase plate of 64% absorption introducing a phase shift of 90° will theoretically enhance contrast from 0 to 0.9 if the phase angle is increased from 0 to 20°. For very small phase angles contrast will even change linearly with φ. This range is most sensitive to changes of phase angle. Maximum contrast is obtained between 30° and 35°. Beyond these values, K drops to 0 at 180° as φ increases. For phase angles between 180° and 360° (negative phase contrast), the curve is inverted. The diagram also shows that even at path differences of up to half a wavelength ($\varphi = 180°$) ambiguous phase images may be produced due to the fact that very different phase angles have the same degree of contrast (25). Thus, for example, a contrast of 0.4 corresponds to phase angles of both 5° and 130°. In practice this means that under the aforementioned conditions points of different optical thickness in the phase object cannot be distinguished because they are of absolutely equal phase contrast.

In order to ensure unambiguous and accurate results, the phase-contrast method should therefore preferably be used for phase objects with small phase angles not exceeding 30°, which is equivalent to a path difference of not more than $\lambda/12$. According to Michel (14, p. 119), thickness differences of $^1/_{100}$ µm (= 10 nm = 100 Å) can still be distinguished with a contrast of 0.3 in a phase object with a refractive index of 1.5; if the geometrical thickness of the phase object is 5 µm, differences of refractive index of 0.001 in the object can be detected.

The above explanation shows that thick specimens are unsuitable for examination by the phase-contrast technique (14, p. 120). The same applies to specimens of wedge-shaped texture: in both cases, the exact reproduction of the annular condenser diaphragm on the phase plate in the microscope objective is made difficult if not impossible (Fig. 5). In these unfavorable conditions, phase contrast loses its experimental basis and becomes more and more of a bright-field method with all the disadvantages this holds for the reproduction of phase objects.

If possible, thin objects should be used also for DIC microscopy. In the case of very thick objects which, moreover, do not lie flat on

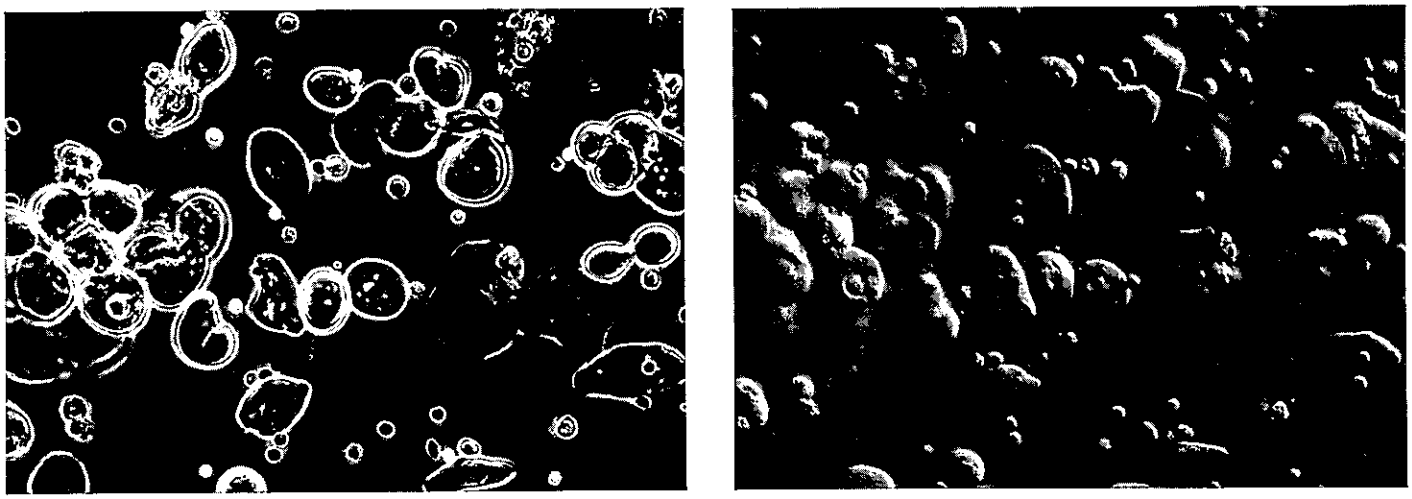

Fig. 7: Reproduction of detail in stratified phase objects. Gynecological smear in a saline solution; immature cells of lower epithelium (basal and parabasal cells). Left: PC image. Right: DIC image. Photomicroscope. 16x N. A. 0.40 Ph-2 Neofluar and 16x N. A. 0.35 Planachromat; Optovar 1.25x. Total magnification approx. 170x.

the specimen slide (Fig. 5), the interference plane of the auxiliary prism in the condenser can no longer be accurately focused on the conjugate interference plane of the principal prism above the objective. For comparison, a thin, flat phase specimen is shown in Fig. 6. In this case, the pupil image of the PC microscope also shows a sharply defined annular condenser diaphragm and objective phase plate; in the DIC microscope, a sharply defined image of the aperture (iris) diaphagm of the condenser is likewise visible in the pupil plane.

A comparison of the photomicrographs published in this journal (27) may serve as an example of the different image quality secured by phase-contrast and differential interference-contrast microscopy. This comparison also shows that the DIC method can be used over a far greater range of path differences in the object than would be practical with the PC method. If in this connection we look at Michel-Lévy's chromaticity diagram, the clear marking of the phase object by interference colors becomes evident over a wide range of path differences. Small path differences of about 50 nm (i. e. approx. $^1/_{10}$ wavelength of green light) fall in the area of first-order gray. The gray tone changes only very slowly with increasing path difference (e. g. up to 100 nm). Inexperienced observers will recognize these changes only with difficulty. In the area of first-order red, however, even slight changes of path difference by about 10 to 20 nm (equivalent to 2 to 4 % of the wavelength of green light) give rise to variations in color which are marked enough to be detected even by inexperienced observers. Since the Nomarski DIC equipment allows one of the Nomarski prisms to be shifted so that the image background can, within certain limits, be made perpendicular to the microscope axis (see 11, 12), phase objects can always be reproduced with optimum contrast.

If Michel-Lévy's chromaticity diagram alone were used to assess the DIC method's suitability for distinguishing optical thickness, the impression might be created that DIC microscopy is suitable only for relatively great path differences (such as 40 nm and larger). However, this is not so. Experience has shown that even very small path differences can be made visible. Fig. 2 may again serve as an example. The extraordinary capabilities of DIC microscopy are probably due to the fact that under favorable conditions[4] phase objects can be reproduced with contrast 1. Owing to this wide range of contrast, the observer is able to detect minor brightness differences and thus differences in optical thickness.

2.5 Gradient of optical thickness

An essential difference between DIC and PC microscopy is due to the lateral variation of optical thickness in a phase object; in this case we also speak of the effect of the gradient of optical thickness on the appearance of the DIC image (1, 8). For better understanding it should be recalled that DIC microscopy may be considered as two-beam interference microscopy with differential shearing (7, 11). If both waves traverse identical optical paths, they will produce identical intensity in the DIC image; in the special case in which the Nomarski prisms are in center position (zero path difference) with polarizer and analyzer crossed, the intensity in the DIC image will be zero. In other words, a variation of intensity (in the aforementioned case, lightening of the DIC image) is possible only if the two waves cover different optical paths. However, since the two waves are separated by only a minute distance – a distance roughly equivalent to the resolution of the microscope – a variation of intensity can occur only if there is a marked change in the optical thickness of the object even over this short distance. Or we may say that the partial differential quotient of the optical path in the phase object as referred to lateral shearing in the DIC system must differ from zero in order to reveal the phase structure of the object in the DIC image. (It is known that no such requirement exists for the phase-contrast technique [see 8].) Naturally, this requirement is easier to satisfy at the edges of objects than in extensive phase objects. It is therefore quite possible that only the boundaries of a phase object will appear in the DIC image. This was explained with a few examples in the discussion of DIC image formation (12, Fig. 4, case A, and Fig. 5, detail I). But it has been found that even the phase-contrast method is not completely free of this complication in regard to image interpretation. For in the DIC image of an extensive phase object of uniform optical thickness the intensity distribution in the interior of the PC object approaches that of the surrounding field, with increasing object size. In an extreme case, the object will therefore only stand out against the background due to the halo effect (26), and it should be noted that the boundary between the bright and the dark fringe is not necessarily identical with the actual limits of the phase structure (see 25).

From a viewpoint of high-fidelity reproduction of phase structures, the aforementioned characteristic of differential interference-con-

[4] By favorable conditions we here understand, for example, a single phase object with relatively few structural details on a homogeneous, i. e. textureless background.

trast microscopy would seem to be a shortcoming. However, it is precisely this apparent drawback which is very helpful in the examination of microscopic objects of greatly varying phase structure, because fine phase detail, which in the PC image passes unnoticed or is seen only with difficulty, occasionally stands out with extraordinary clarity in the DIC image (see Fig. 7, bottom). This is due to the above mentioned fact that in the DIC image the intensity distribution is determined by the difference in path length between the (plane) reference wave and the (deformed) differential wave (12). This explains why even with heavily structured object fields of greatly varying optical thickness the background will appear fairly plane ("flat"). Local optical path differences stand out with apparent relief from this "plane".

2.6 Depth of field

An essential advantage of Nomarski DIC microscopy over PC microscopy is due to the shallow depth of field involved in this method. We know that in the PC system the illuminating (and viewing) aperture is determined by the dimensions of the PC attachment; it cannot be varied. In Nomarski DIC microscopy, on the other hand, the diameter of the aperture diaphragm in the condenser can easily be adapted to the requirements of the specimen (1), as in bright-field work. A relatively large aperture (about $^2/_3$ of the objective aperture) can generally be used without any loss of contrast. Owing to this high illuminating aperture, the DIC method offers only shallow depth of field, which is particularly welcome for thick objects. Details outside the focal plane are thus less disturbing in the microscopic image than in phase contrast (see Fig. 2). As a result, DIC images of excellent quality can be obtained even under unfavorable conditions when PC images – due to their great depth of field – make the identification of phase structures impossible because of overlapping details above and below the objects of interest and, in addition, due to the halo effect. Here again, the bottom portion of Fig. 7 may serve as an example (see also 23).

2.7 Dichroic objects

One source of errors in the DIC method is the necessity of using polarized light. We can distinguish between an ordinary and an extraordinary ray, as was described in the preceding parts of this paper (11, 12). In so-called dichroic objects, the ordinary and extraordinary rays are absorbed to different degrees. In other words, they interfere with different intensity so that the DIC image is not only a function of the difference of optical path length for the two rays, which would normally be of interest, but also of the different absorption in the two beams. This effect is comparable to a setup in which the planes of transmission of polarizer and analyzer are not perfectly perpendicular to each other (see 12). Phase contrast, on the other hand, does not require the use of polarized light. Consequently, the PC method is free from possible disturbance due to dichroic substances. It may generally be said that in practice it will only rarely be necessary to examine dichroic (i. e. absorbing) objects with microscopes designed for phase work.

3. Summary

In addition to the outstanding features of the ZEISS DIC accessories explained in this series of papers on Nomarski DIC microscopy there are quite a number of aspects which cannot be discussed here. Apart from these theoretical considerations, practical experience also advises against the classification of the Nomarski DIC method at this stage, because it has been found that Nomarski DIC microscopy is being used increasingly in fields in which conventional methods of light microscopy have failed or give only unsatisfactory results.

However, we already know beyond any doubt that Nomarski DIC microscopy has gained a firm footing in reflected-light microscopy because it is clearly superior to incident phase-contrast microscopy in a great number of cases. In transmitted-light microscopy, on the other hand, the two methods would appear, as before, to complement each other. This once more justifies the ZEISS concept of combining annular diaphragms for PC microscopy with auxiliary Nomarski prisms for DIC microscopy in the type V Z achromatic-aplanatic substage condenser.

It is also noteworthy that the PC and DIC accessories by ZEISS differ in one essential point: The ZEISS phase-contrast systems are equipped with phase plates for constant phase shift and constant absorption. The ZEISS Nomarski DIC systems, on the other hand, allow both the phase of the light and its amplitude to be varied (the former by adjusting one of the Nomarski prisms, the latter by moving the analyzer out of its crossed position in relation to the polarizer). If in spite of this the phase-contrast technique has lost hardly any of its importance, this is probably due to two reasons:

a) Phase-contrast techniques are primarily used for the examination of biological and medical objects, and
b) biological and medical phase objects generally vary so greatly in local optical thickness that it would be neither reasonable nor possible to obtain optimum contrast at every point in the entire phase object by means of a variable phase-contrast system (see 14, p. 117). A compromise solution will thus be inevitable in these cases.

However, the situation is apparently quite different in reflected-light microscopy. Here the microscopic objects to be examined are "plane" from the start, and their relief varies only within relatively narrow limits. (With transparent objects, this relief is equivalent to geometrical thickness.) A second variable is then the locally different phase retardation upon reflection of the incident light from the surface of the opaque object. (In the case of transparent objects, the refractive index has to be taken into account instead.) Contrary to transparent objects, the interesting detail in opaque objects is frequently a small phase object on a homogeneous phase background. In this case, an extremely useful feature of the Nomarski DIC system is the fact that by suitable selection of path difference with the aid of one of the Nomarski prisms the object can be made to stand out optimally from the surroundings by means of interference (see 8). With biological objects, however, the range within which path-difference staining can be used is considerably smaller; it is limited to fractions of a wavelength (usually below $\lambda/4$). This is why in the case of (biological) transparent specimens the need of a microscopic method allowing variable staining is by far less pressing than with (non-biological) opaque objects.

References

[1] *Allen, R. D., G. B. David* and *G. Nomarski:* The ZEISS-Nomarski Differential Interference Equipment for Transmitted-Light Microscopy, Z. wiss. Mikr. (at press)

[2] *Barer, R.:* Phase Contrast, Interference Contrast, and Polarizing Microscopy, in Analytical Cytology. (Pub. R. C. Mellors) McGraw-Hill Book Comp., New York 1955

[3] *Barer, R.:* Phase Contrast and Interference Microscopy in Cytology, in Physical Techniques in Biological Research (Pub. G. von Oster und A. W. Pollister), Academic Press, New York 1956, S. 29

[4] *Beyer, H.:* Theorie und Praxis des Phasenkontrastverfahrens, Akad. Verlagsgesellschaft Frankfurt am Main 1965

[5] *Françon, M.:* Le contraste de phase en optique et en microscopie, Paris 1951

[6] *Françon, M.:* Le microscope à contraste de phase et le microscope interferentiel, Paris 1954

[7] *Françon, M.:* Einführung in die neueren Methoden der Lichtmikroskopie, übersetzt von L. Albert, Verlag G. Braun, Karlsruhe 1967

[8] *Gabler, F.* und *F. Herzog:* Eine neue Interferenzkontrasteinrichtung für Arbeiten im Durchlicht, Druckschrift SD Interf. Kontr. DL D 8/66 bzw. SD Interf. Kontr. DL E 2/67

[9] *Haselmann, H.:* 20 Jahre Phasenkontrastmikroskopie, Historischer Rückblick und aktuelle Sonderfragen, Z. wiss. Mikrosk. **63** (1957) 140

[10] *Haselmann, H.:* Phasenkontrast-Mikroskopie, Betrachtungen zur Entwicklung einer wissenschaftlichen Apparatur, ZEISS-Werkzeitschrift 5 Vol. 26 (1957) S. 109

[11] *Lang, W.:* Differential-Interferenzkontrast-Mikroskopie nach Nomarski, Teil I: Grundlagen und experimentelle Ausführung, ZEISS Information Vol. 70 (1968) 114

[12] *Lang, W.:* Differential-Interferenzkontrast-Mikroskopie nach Nomarski, Teil II: Entstehung des Interferenzbildes. ZEISS Information Vol. 71 (1969) 12

[13] *Michel, K.:* Die Grundzüge der Theorie des Mikroskops in elementarer Darstellung, 2. Aufl., Bd. I der Reihe Physik und Technik, Herausgeber F. Gößler, Wissenschaftliche Verlagsgesellschaft mbH., Stuttgart 1964

[14] *Michel, K.:* Die Mikrophotographie, 3. Aufl., Bd. X der Reihe „Die wissenschaftliche und angewandte Photographie", Pub. J. Stüper, Springer-Verlag Wien-New York 1967

[15] *Menzel, E.:* Phasenkontrast-Verfahren, Z. f. angew. Phys. **3** (1951) 308

[16] *Menzel, E.:* Phasenkontrast-Verfahren, in Hdb. d. Mikroskopie in der Technik (Pub. H. Freund), Vol. I, Part 1, Frankfurt a. Main 1957

[17] *Neupert, H.:* Interferenzkontrast-Einrichtung nach Nomarski (Lizenz CNRS), ZEISS Information Vol. 65 (1967) 96

[18] No author: Supplement to catalog S 40-554 of CARL ZEISS

[19] *Nomarski, G.:* Interféromètre à polarisation, Brevet français No. 1 059 123, 1952

[20] *Nomarski, G.:* Microinterféromètre differentiel à ondes polarisées, J. Phys. Radium, Paris **16** (1955) 9

[21] *Nomarski, G.* et Mme. *A. R. Weill:* Application à la métallographie des méthodes interférentielles à deux ondes polarisées, Rev. Métallurg. **52** (1955) 121

[22] *Osterberg, H.* and *O. W. Richards:* Phase microscopy, New York, London 1951

[23] *Padawer, J.:* The Nomarski interference-contrast microscope. An experimental basis for image interpretation. J. Roy. Micr. Soc. **88** (1968) 305

[24] *Richter, R.:* Eine einfache Erklärung des Phasenkontrastmikroskops, Optik **2** (1947) 342

[25] *Rienitz, J.:* Phasenkontrastverfahren, in „ABC der Optik" (Pub.: K. Mütze, L. Foitzik, W. Krug und G. Schreiber), Verlag Werner Dausien, Hanau/Main 1961

[26] *Wolter, H.:* Schlieren-, Phasenkontrast- und Lichtschnittverfahren in Hdb. d. Physik (Pub. S. Flügge) Vol. 24, Berlin, Göttingen, Heidelberg 1956

[27] *Wunderer, A.* und *S. Witte:* Zur Anwendung der Interferenzkontrastmikroskopie in der Zytologie, ZEISS Information Vol. 70 (1968) 121

[28] *Zernike, F.:* Das Phasenkontrastverfahren bei der mikroskopischen Beobachtung, Z. Phys. **36** (1934) 848

[29] *Zernike, F.:* Das Phasenkontrastverfahren bei der mikroskopischen Beobachtung, Z. techn. Physik **16** (1935) 454

IV. Applications

In the comprehensive description of Nomarski differential interference-contrast (DIC) microscopy, the fundamentals and experimental designs (Part I) and the formation of the interference image (Part II) were discussed and a comparison made with the phase-contrast technique (Part III) [26, 27, 28]. The present Part IV will now give a review of the applications of Nomarski DIC microscopy together with a list of references. No claim is made with regard to the completeness of the bibliographic data in view of the rapidly increasing number of applications and publications on the subject. The bibliography is therefore only intended to serve as a guide to the potential uses of the Nomarski DIC method in the different fields of microscopy of organic and inorganic objects.

A. Microscopy of organic objects

An essential advantage of Nomarski DIC microscopy is the fact that – like phase contrast, for example – it allows the examination of unstained specimens. A new and extremely useful aid has thus been created, above all for examining living specimens under the optical microscope.

Cytology

Using a living cell of Haemanthus katherinae in the process of division as an example, *Bajér* and *Allen* [5] demonstrate the superiority of the DIC image over phase-contrast representation: while in phase contrast the halo effect makes it impossible to recognize details, the spindle fibers can be clearly seen by the Nomarski differential interference-contrast method.

DIC micrographs of hela cells in a nutrient solution and denatured with 96% alcohol were published by *Gabler* and *Herzog* [18, 19].

Wunderer and *Witte* [47] published a comparison of photomicrographs of cells and groups of cells from the mucuous membrane of the human stomach, taken by phase contrast and by Nomarski differential interference contrast. These examples prove that the two methods complement each other very nicely. However, in the case of a group of glandular cells of the gastric mucosa, the interference method offers the advantage of improved detail definition.

Giving many practical examples, *Padawer* [39] explains the characteristics and advantages of DIC microscopy. In a "rat peritoneal-fluid cell", for instance, nuclei and vacuoles appear in the DIC image as depressions, while highly refractive structures such as eosinophile granula or fatty inclusions seem considerably elevated. Also, the vacuoles of macrophages appear as depressions, while the nuclear membrane shows up as a bulge. The author shows that phase structures located outside the focal plane cannot always be neglected in the interpretation of DIC images. When erythrocytes are viewed by phase contrast, the formation of haloes is rather troublesome. In this case, the DIC image is unmistakably superior. The situation is similar with epithelial cells of the mucuous membrane of the human mouth.

Duitschaever [14] uses the DIC method for microscopic investigations on somatic cells in cow's milk and other body fluids. *Engels* and *Ribbert* [15] also use Nomarski differential interference contrast for the examination of nucleoli in Musca domestica. *Ribbert* and *Bier* [41] make use of the Nomarski method for studying insect ovaries.

Stoll * and *Gundlach* [43] compare the phase-contrast image with the DIC image of a cell smear in a saline solution. The living trichomonad beside an epithelial cell and erythrocytes shows more detail in interference contrast. This holds true, above all, for the marginal portions of the trichomonad which in phase contrast reveal considerable flare due to halation. A similar situation is encountered in the case of the basal and parabasal cells of a gynecological cell smear in a saline solution. This example also shows that it is easier to distinguish superimposed structures in the DIC image than in phase contrast. The authors prove that in such a case it is frequently impossible to recognize the borders of the cell in phase contrast due to halation.

Botany

The phase-contrast technique is well suited for examining small particles – especially organelles – in protoplasm [44]. However, the great depth of field of this method is a disadvantage in botany. As a result, phase structures in the light path will impair the phase image even if they are located outside the focal plane [44]. According to *Url* and *Gabler* [44], the shallower depth of field of Nomarski DIC microscopy opens up a considerably wider field of application for light microscopy in botany. These authors show, among others, DIC micrographs of the inside and outside epidermis of Allium cepa, cells of Closterium lunula and – in a comparison with phase contrast – Micrasterias denticulata and Closterium lunula. In the case of Allium cepa, mitochondria, the Golgi complex, leucoplasts, the nucleolus and large and small spherosomes stand out in high contrast, the latter due precisely to the great difference between their own refractive index and that of the surrounding area.

According to *Padawer* [39], observation of plant material offers considerable difficulty, be it in phase contrast or differential interference contrast. In the one case, the pronounced difference of refractive index gives rise to heavy halation, in the other, birefringent components disturb the image. This has been proven for example in the case of dried pollen such as Salix discolor and, above all, Coreopsis. Similar conditions are encountered with freshwater Chlorophyceae. *Maguire* [29] investigates subchromatid structures in corn with the aid of the Nomarski method and, for comparison, in phase contrast.

Using Haemanthus katharinae as an example, *Allan, David* and *Nomarski* [3] show that the spindle fibers of a living cell during division stand out clearly in the DIC image (see also [5] and [6]), whereas they are hardly visible by any other microscope technique.

---

* See the monograph meanwhile published by Peter Stoll: Gynecological Vital Cytology in Practice, Springer-Verlag Berlin, Heidelberg, New York 1969, which contains numerous practical examples of DIC microscopy, often with comparative phase-contrast micrographs.

Histology

Gabler and *Herzog* [18, 19] show the thyroid gland of a mouse in positive and negative phase contrast as well as in Nomarski differential interference contrast. Nomarski DIC is also suited for amplitude staining of stained specimens, as shown by *Allan, David* and *Nomarski* [3] on large chromosomes of Drosophila melanogaster. Even human chromosomes can easily be examined by the DIC method using amplitude staining. Very thick bone sections as generally used, for example, for examination by incident fluorescent illumination, result in a noticeable decrease in contrast in the DIC image, as in phase contrast. This is due to the fact that proper imaging of the contrast-producing components, such as annular diaphragm on phase plate or auxiliary prism on principal prism, is no longer guaranteed. This is demonstrated by *Lang* [28] both for phase contrast and Nomarski differential interference contrast by the example of an excessively thick transparent specimen (polished bone section) and a thin, well-suited transparent specimen (rat's tongue, unstained).

In spite of this reservation, the Nomarski DIC method is ideally suited for optical sectioning in view of its high useful aperture and the resulting shallow depth of focus. This is amply shown by an example from the field of zoology. Fig. 1 combines photomicrographs of Macronyssus bacoti taken in bright field (a), phase contrast (b) and Nomarski differential interference contrast in one and the same focal plane. In addition, the micrographs d and e show another two planes of the same object in differential interference contrast.

The assessment of thin sections is considerably facilitated by the Nomarski DIC method, as is borne out by the comparison with bright field viewing shown in Fig. 2. In this type of work the DIC method can also be used to advantage for stained specimens. The color distortion introduced in this case by the Nomarski method remains within acceptable limits. In addition, it should be remembered that for the purpose of comparison rapid and convenient change-over to bright-field viewing is possible, e. g. by removing the Inco slide from the light path.

Hematology

With the aid of Nomarski DIC microscopy, unstained erythrocytes can be rendered visible with excellent results [18, 19]. According to the authors, the DIC image of a crystal in the blood lymph of an eel is superior to the corresponding phase-contrast image that is impaired by halation.

Padawer [39] discusses differences between phase-contrast and differential interference-contrast observation of the hemolysis of frog erythrocytes.

The photomicrographs taken under identical conditions show non-hemolyzed cells, spherocytes and completely hemolyzed cells. The author shows that with normal cells the nucleus in the DIC image stands out more clearly from the cytoplasm than in phase contrast. The nucleus becomes more elevated from the cytoplasm, the more water the cell absorbs and the more hemoglobin it loses. With completely hemolyzed cells, the cytoplasm will show up only weakly due to the loss of hemoglobin, while the nucleus stands out in good contrast. In another case, a fresh blood smear, the coiling makes phase-contrast observation impossible due to heavy halation. In the DIC image, however, sufficient detail can be recognized in spite of the stratification. In phase contrast, fibrin fibers may appear dark or bright, depending on whether or not they lie in the focal plane. This complication does not exist in differential interference contrast.

Neurology

Neuhoff [31] uses Nomarski DIC microscopy to render human ganglion cells visible and especially for examining cells in which an appendix leads back to the same cell, so-called feedback neurons.

Bacteriology

With bacteria specimens, the disturbing halation known from phase-contrast images presents an advantage in Nomarski DIC microscopy; as an example, *Gabler* and *Herzog* [18, 19] show a smear of Klebsiella.

Hydrobiology

Quite a number of authors have published DIC photomicrographs of diatoms which show up 3-dimensionally in the DIC image. Due to the excellent resolution of the Nomarski DIC method, minute detail can be recognized in the diatoms.

Gabler and *Herzog* [18, 19] show the DIC image of Auliscus sculptus.

The use of Nomarski DIC microscopy in micropaleontology is described by *Barbieri* and *Mazzola* [7].

Padawer [39] compares phase-contrast and differential interference-contrast images of various diatoms. In this comparison, the superiority of the DIC image becomes very evident.

In a very comprehensive paper, *Allen, David, Hirsh* and *Watters* [2, 13] cover the subject of image interpretation in transmitted-light polarizing interference microscopes both of the image-duplication and the differential type. In addition to an extensive comparative discussion of theoretical and experimental principles, the differences are illustrated impressively by a number of practical examples. Under Nomarski even large path differences of up to $2\,^1/_4\ \lambda$ between Staurоneis acuta diatoms and the mounting medium give images that are rich in detail. The Durirella robusta diatom can be reproduced with good contrast even with an illuminating aperture of 1.25. As a result, object details that are invisible at a smaller numerical aperture of, for example, 0.6, can be clearly distinguished.

Allan, David and *Nomarski* [3] report on the fundamentals, design, function and characteristics of ZEISS differential interference-contrast equipment. A number of practical examples explaining the special features of the equipment concern diatoms: Staureonis acuta diatoms in the DIC image as compared to the interference-contrast image (photographed with the ZEISS Jamin-Lebedeff system) show that particularly pronounced gradients of optical thickness in the specimen are reproduced very clearly in the DIC image. The azimuth effect of the technique can be demonstrated very impressively in the Hantzschia amphioxys diatom. Radial structures such as Anachnodicus ehrenbergii diatoms also reveal the azimuth effect. Using the example of the Surirella robusta diatom, the authors explain the advantage of DIC equipment over bright-field and phase-contrast observation, in that excellent contrast is obtained even at high aperture. In other words, the Nomarski DIC method has the effect of a filter that amplifies high spatial frequencies and subdues low ones. The advantage of the shallow depth of field of the DIC method as compared to phase contrast is illustrated by a Triceratium favus diatom.

B. Microscopy of inorganic objects

Metallography

As early as 1954, *Nomarski* and Mme *Weill* [32] pointed out the advantages of differential interference-contrast microscopy in the field of metallography (e. g., electropolished cobalt). A second publication by the same authors [33] dealt exclusively with metallographic applications. Among other things, it was devoted to a detailed study of various growth spirals of SiC. Nomarski and Mme Weill were able to prove that growth steps of 440 Å ± 30 Å, for example, can be resolved without difficulty. Under certain conditions, a relief of the order of magnitude of a few Angstrom units can be recognized in the DIC image. Slipbands in cobalt subjected to a tension of 440 g/mm^2 for a period of five minutes can be reproduced with excellent contrast. The photomicrographs show various patterns of slipbands which, with bright-field illumination, for instance, can be recognized only with difficulty or not at all.

Measuring thin films of an order of magnitude of 2000 Å with the aid of yellow sodium light (589 mμ) and a Nomarski differential interference equipment, Le *Méhauté* [24] obtains an accuracy of ± 1.5 %. The author comes to the conclusion that the DIC method is superior to bright-field and particularly to phase-contrast observation for

testing highly polished surfaces, examining thin films on glass substrates (vacuum-deposited films), checking quenched steel for undesirable phases such as ferrites, austenites, etc., and finally for the testing of diffusion processes by phase changes, the creation of new phases, recrystallization or other defects such as porosity due to different rates of diffusion between two elements, and lastly checking for dislocations and displacement of grain boundaries. As practical examples Le Méhauté publishes photomicrographs of quenched Cr-Ni-Mo steel, cold-worked bronze and sintered iron.

Bertocci and *Noggle* [9] use a differential interference-contrast system for the quantitative examination of small etched copper surfaces down to a mean size of 6 μ. Depending on the magnification of the objective used, they attain an accuracy of between $\pm$ 5′ and $\pm$ 30′.

The superiority of Nomarski DIC microscopy over bright-field observation is illustrated by *Gahm* [20] who compares photomicrographs of unalloyed quenched and tempered steel taken under both techniques. The deformation of the surrounding area produced by a microhardness indenter, of which no trace is visible in bright field, can be clearly distinguished in the DIC image. At the same time, the series of micrographs shows the azimuth effect characteristic of the Nomarski DIC method, which can here be observed along a linear grinding trace. *Jeglitsch* and *Mitsche* [23] use Nomarski to investigate the metallographic structure of Vacutherm samples (Widmannstätten structures, ferrite after 8/α-conversion, pearlite containing 0.85 % C), of low-temperature martensite, white cast iron (hypereutectic and hardened) and fused high-speed steel.

On the left, Fig. 3 shows a martensite needle magnified 800 x in bright field, on the right, the same needle in Nomarski differential interference contrast.

Crystallography

In 1954 *Nomarski* and Mme *Weill* [32] reported numerous practical examples and illustrated the use of Nomarski DIC microscopy in crystallography, e. g. growth spirals on silicon carbide (SiC) with triangular symmetry; principal spirals with secondary recrystallization on SiC; star-shaped growth spirals, etc.

Using the example of microhardness indentations in cleavage surfaces of sodium-chloride crystals and potassium-chloride crystals, *Gahm* [20] shows that DIC microscopy can be used to advantage for quantitative investigations. Slipbands that cannot be recognized under bright-field illumination stand out with extraordinary clarity in the DIC image.

The superiority of the Nomarski DIC method over phase contrast is clearly evident from the replica of a calcite cleavage surface [18, 19].

Padawer [39] compares sodium-chloride crystals in bright field, phase contrast and differential interference contrast. In bright field practically only the contours of the crystals will become visible, even if the illuminating aperture is reduced, and in the phase-contrast image large parts of the object will be veiled by halation. However, in the DIC image, even points of only minor path difference can be clearly distinguished.

For the optical staining and examination of the surfaces of germanium and silicon dioxide, *Françon* [17] takes recourse to reflected-light differential interference contrast. However, ammonium-alum crystals can be reproduced with a wealth of detail by optical staining even when transmitted light is used.

Mineralogy

Gahm [20] has successfully used Nomarski DIC microscopy to make microhardness impressions in various minerals (e. g. covellite, Boulangerite) visible. Cracks, scabbiness and bulges around a microhardness indentation in a periclase cleavage surface can be made optimally visible by color contrast.

Von Gehlen and *Piller* [21] have shown that Nomarski DIC microscopy is an ideal means for examining polished specimens or ore minerals for hardness differences. This method has proved to be superior to the conventional "Schneiderhöhn line". Moreover, the Nomarski method is a valuable aid in testing the quality of polished surfaces whose reflectivity is to be measured by microphotometry. Finally, with substage illumination the Nomarski method offers many advantages for assessing the morphographic properties of fine-grain minerals and identifying clay minerals, as *Correns* and *Piller* [11] have shown.

Semiconductor technology

In the introduction to his paper, *Le Méhauté* describes the fundamentals and characteristics of the Nomarski differential interference-contrast method and continues by giving a summary of its advantages over bright-field and phase-contrast observation, particularly for metallographic uses. In the semiconductor field, the DIC technique may be used to advantage for observing structural changes such as phase transitions, the formation of new phases, recrystallization processes, etc. Le Méhauté shows that the DIC image of a transistor reveals far more detail than would a bright-field image.

Besides a comprehensive and easily understandable introduction to Nomarski DIC microscopy, *Françon* [17] publishes a number of photomicrographs of a germanium surface, a micro-circuit and a cadmium-tellurite film on silicon dioxide.

Owing to its high resolution, the Nomarski method is well suited for the examination of silicon monocrystals, as has been shown by *Vieweg-Gutberlet* [45]. If the specimens are properly etched, inhomogeneities in the dopant concentrations – such as striations, the microstructures of striations, stacking faults in concentrations, etc. – can be made visible. Fig. 4 shows a wafer in bright field (left) and in Nomarski differential interference contrast (right).

Fig. 5 shows a cross-section of an integrated circuit that failed due to overload, on the left in bright field and on the right in DIC. Differential interference contrast above all reproduces the conductors with greater detail.

Glass technology

Minute details in a glass surface are reproduced with high contrast in the DIC image. As is proved by *Gabler* and *Herzog* [18, 19], pronounced differences of refractive index between object and mounting medium which, in phase contrast, result in extremely disturbing haloes, do not have the same unfavorable effect in the DIC image. When examining oriented linear phase structures, their orientation relative to the splitting direction of the Nomarski prisms must be taken into account [28]. The phase-contrast technique has no inherent azimuth effect. However, it has the disadvantage of greater depth of field so that phase objects lying outside the focal plane will appear in the image, for example, as disturbing diffraction fringes.

Plastics

Like clear transparent glass, clear transparent plastics are ideal phase objects. According to *Gahm* [20], microhardness impressions or extremely minute irregularities that are invisible in bright field can be emphasized by suitable setting of the background, above all in color contrast.

A comparison between the optical staining of spherical plastic parts in dark field and differential interference contrast is made by *Padawer* [39]. This comparison proves the advantages of the DIC method by which even very small particles are clearly reproduced beside larger objects. With the aid of polystyrene spheres with a mean diameter of 1.3 μ, mounted in glycerin, *Padawer* demonstrates the dependence of the DIC image on the illuminating aperture. The optimum illuminating aperture depends both on the object and the illuminating aperture. In the special case under discussion, a setting of 75 % of the maximum aperture has proved particularly favorable. In addition, with the aid of two photomicrographs, the author explains the effect of defocusing on the DIC image. A number of micrographs of plastic spheres shows that diffusion processes within the particles, involving a variation of optical thickness, can be clearly reproduced by differential interference contrast.

1 a

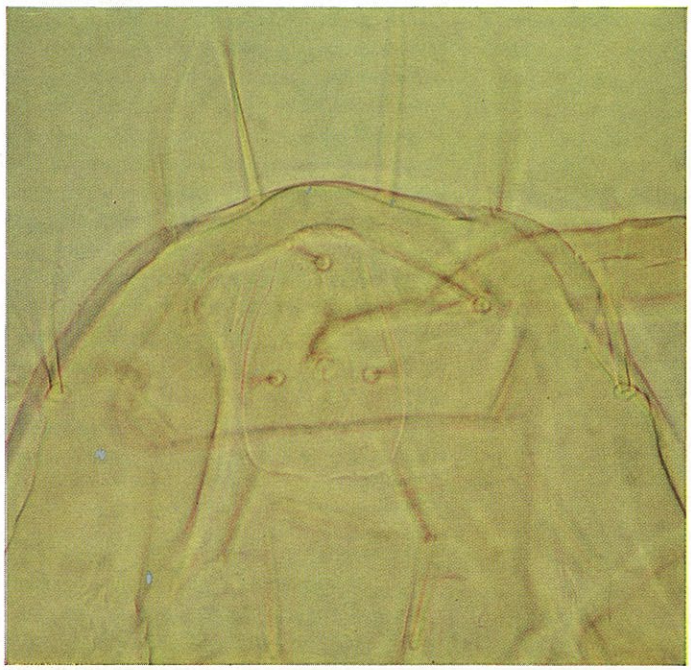

1 b

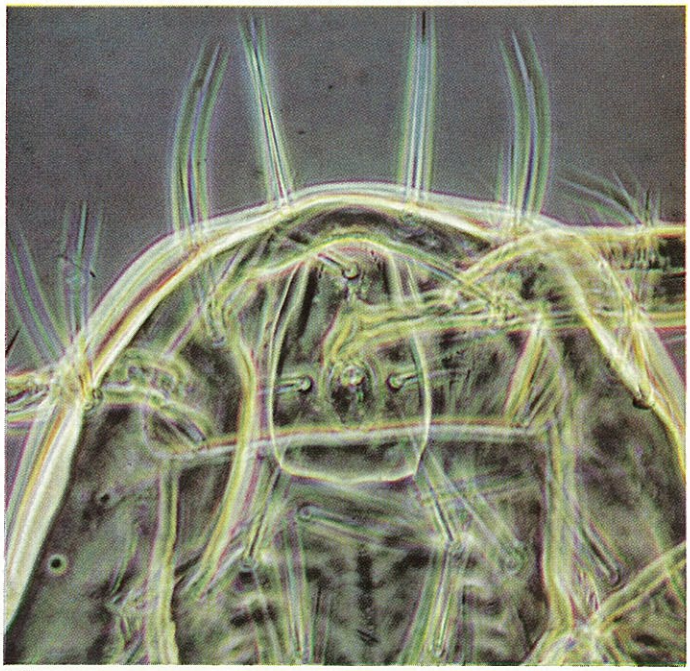

1 c

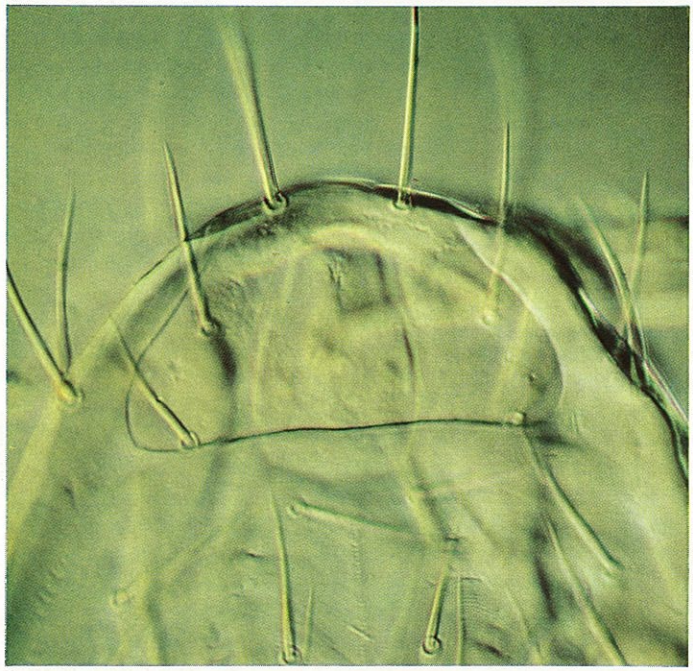

1 d

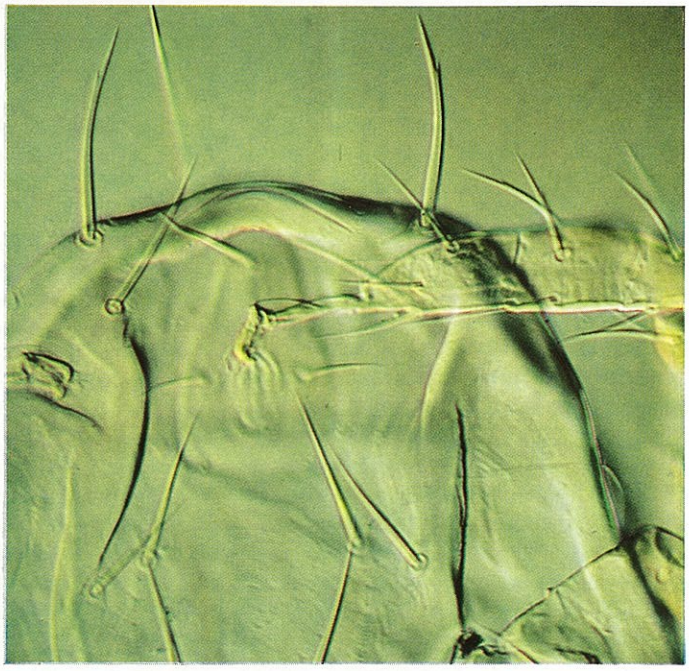

1 e

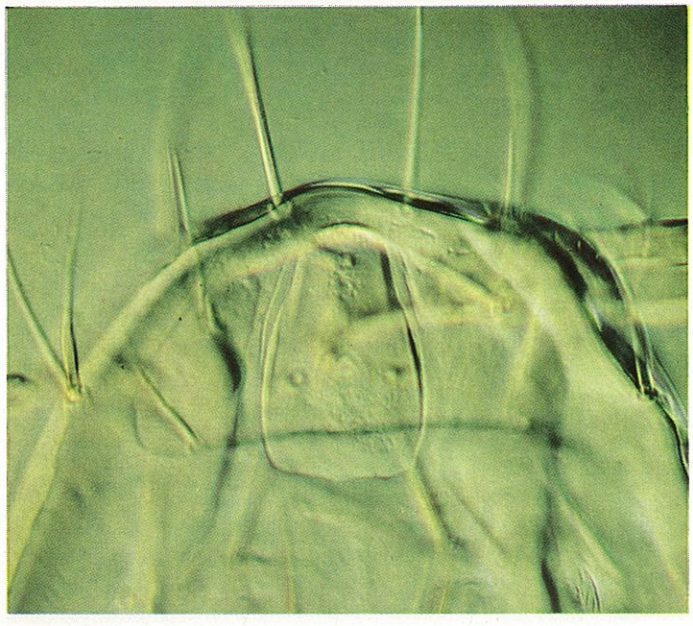

Fig. 1: Macronyssus bacoti in bright field (a), phase contrast (b) and differential interference contrast (c, d, e). Micrographs d and e were focused for different planes. ZEISS Ultraphot II, 40 x N.A. 0.65 Planachromat, magnification 320 x.

2 a

2 b

5 a

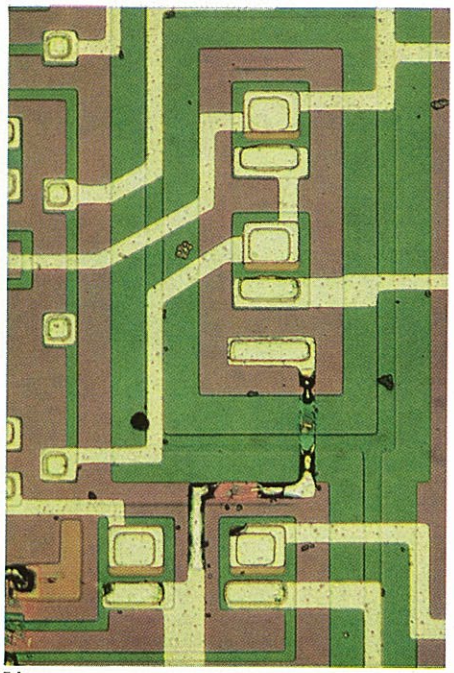

3 a

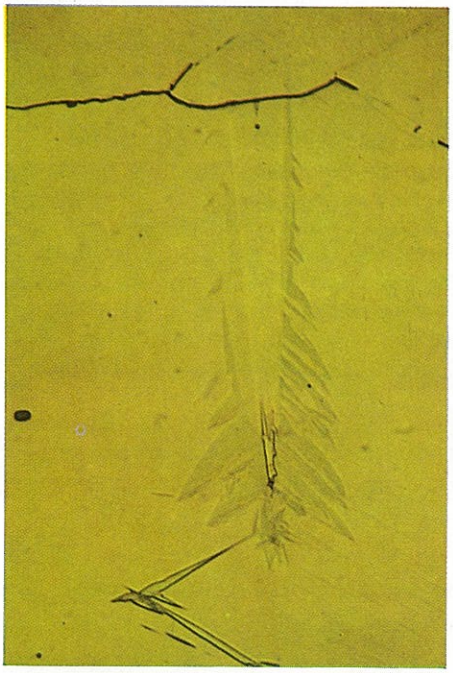

3 b

5 b

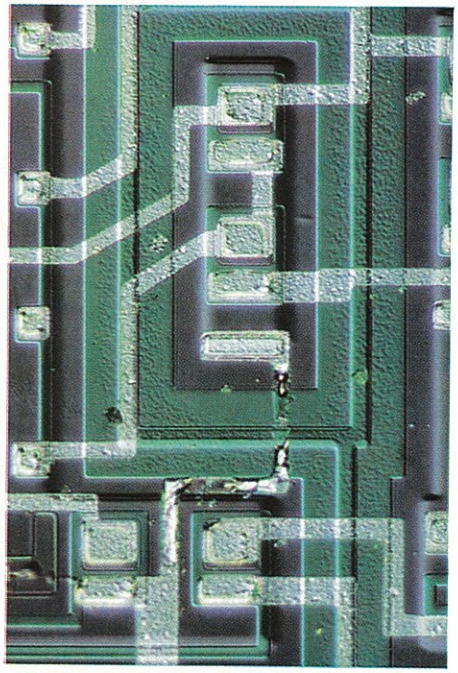

4 a

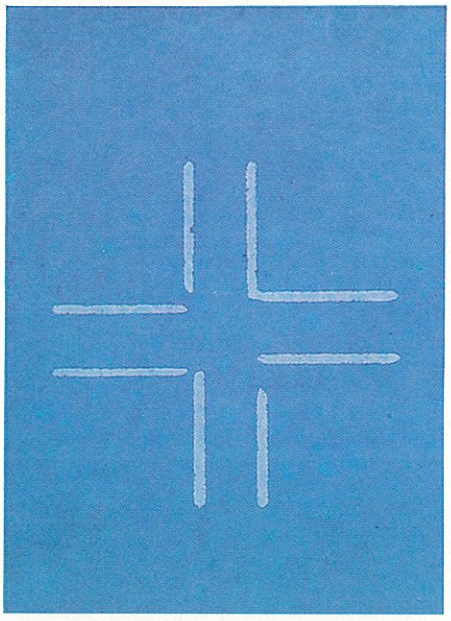

4 b

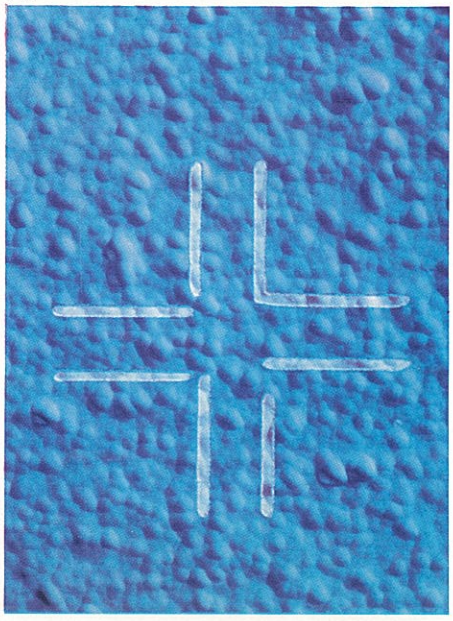

Fig. 2: Cat muscle, left: bright-field, right: Nomarski DIC method. ULTRAPHOT II, 16 x, N.A. 0.35 Planachromat, magnification 144 x.

Fig. 3: Martensite needle, left: bright field, right: Nomarski DIC. ULTRAPHOT II, 100 x Epiplan, N. A. 1.25, oil, magnification 800 x.

Fig. 4: Wafer; bright field (left) and Nomarski DIC micrograph (right). ULTRAPHOT II, 8 x Epiplan, N. A. 0.2, magnification 72 x.

Fig. 5: Cross-section of an integrated circuit. Bright field (above) and Nomarski DIC (belowe). ULTRAPHOT II, 8 x Epiplan, N.A. 0.2, magnification 72 x.

References

[1] *Allen, R. D., G. B. David,* and *L. F. Hirsh jr.:* Proc. R. micr. Soc. 1 (1966) 141

[2] *Allen, R. D., G. B. David, L. F. Hirsh jr.,* and *C. D. Watters:* I. Contrast Generators in Modified Polarizing Microscopes and the Sources of Contrast

[3] *Allen, R. D., G. B. David,* and *G. Nomarski:* Z. wiss. Mikr. 69 (1969) 193

[4] *Bajér, A.:* J. Cell. Biol. 27 (1965) 7A

[5] *Bajér, A.,* and *R. D. Allen:* Science, N.Y., 151 (1966) 572

[6] *Bajér, A.,* and *R. D. Allen:* J. Cell. Sci. 1 (1966) 455

[7] *Barbieri, F.,* and *S. Mazzola:* Acta Naturalia IV (1968) Fasc. 2

[8] *Baum, B. R.:* Canadian Journal of Botany 47 (1969) 85–91

[9] *Bertocci, U.,* and *T. S. Noggle:* Rev. Sci. Instr. 37 (1966) 1750

[10] *Bessis, M.,* and *J. P. Thiéry:* Revue Hématol. 12 (1957) 518

[11] *Correns, C. W.,* and *H. Piller:* Hdb. d. Mikroskopie in der Technik (Handbook of microscopy in technology), Vol. 4, Part 1, edited by H. Freund, 2nd edition (in preparation), Umschau-Verlag Frankfurt

[12] *David, G. B., R. D. Allen, L. F. Hirsh jr.,* and *C. D. Watters:* Proc. R. micr. Soc. 1 (1966) 142

[13] *David, G. B., R. D. Allen, L. F. Hirsh jr., C. D. Watters:* II. The Instrumental Extinction Factor, The Control of Contrast, and Limits of Sensitivity

[14] *Dultschaever, C. L.:* Mikroskopie 23 (1968) 345

[15] *Engels, W.,* and *D. Ribbert:* Experientia 25 (1969)

[16] *Everingham, J. W.:* Anato. Rec. 157 (1967) 242

[17] *Françon, M.:* Bild der Wissenschaft, February issue (1969) 147

[18] *Gabler, F.,* and *F. Herzog:* Leaflet SD. Interf. Kontr. DL D 8/66 of Messrs. C. Reichert, Optische Werke AG, Vienna

[19] *Gabler, F.,* and *F. Herzog:* Leaflet SD. Interf. Kontr. DL E 2/67 of Messrs. C. Reichert, Optische Werke AG, Vienna

[20] *Gahm, J.:* ZEISS Information No. 62 (1966) 120 (Reprint S 40-650), see also 41-700

[21] *Gehlen, K. v.,* and *H. Piller:* Mineralogical Mag. 35 (1965) 335–346

[22] *Grimbert, L.,* and *G. Pigeat:* Archs. oral. Biol. 6 (1961) 139

[23] *Jeglitsch, F.,* and *R. Mitsche:* Radex-Rundschau, No. 3/4 (1967) 587–596

[24] *Le Méhauté, C.:* IBM Journal, April 1962, 263–267

[25] *Lettré, H.:* Path. Biol., Paris 9 (1961) 817

[26] *Lang, W.:* ZEISS Information No. 70 (1968) 114–120 (Reprint S 41-210.2)

[27] *Lang, W.:* ZEISS Information No. 71 (1969) 12–16 (Reprint S 41-210.3)

[28] *Lang, W.:* Reprint S 41-210.4

[29] *Maguire, Marjorie P.:* Proc. nat. Acad. Sci. (Wash) 60 (1968) 533–536

[30] *Author unknown:* Leaflet K I – III D 6/60 of Messrs. C. Reichert, Optische Werke AG, Vienna

[31] *Neuhoff, V.:* Die Naturwissenschaften 54 (1967) 287

[32] *Nomarski, G.,* and *Mme. A. R. Weill:* Bull. Soc. Franç., Minér. Crist. 77 (1954) 840

[33] *Nomarski, G.,* and *Mme. A. R. Weill:* Revue de Metallurgie 52 (1955) 121

[34] *Nomarski, G.:* Revue Hématol. 12 (1957) 439

[35] *Padawer, J.:* Anat. Rec. 151 (1965) 499

[36] *Padawer, J.:* Proc. VIIIth Int. Congr. Anat. Wiesbaden, p. 91, Georg Thieme Verlag, Stuttgart

[37] *Padawer, J.:* Proc. Soc. Exp. Biol. Mech. 120 (1965) 318

[38] *Padawer, J.:* J. Cell. Biol. 29 (1966) 176

[39] *Padawer, J.:* J. Roy. Microsc. Soc. 88 (1968) 305

[40] *Pinet, J.:* Res. Film 4 (1961) 30

[41] *Ribbert, D.,* and *K. H. Bier:* Chromosoma 27 (1969) 178–197

[42] *Robineaux, R.:* Res. Film 3 (1959) 138

[43] *Stoll, P.,* and *H. Gundlach:* Private communication. The photomicrographs made available were published in 28. Recently published: *Stoll, P.:* Gynecological Vital Cytology in Practice, Springer-Verlag Berlin, Heidelberg, New York 1969

[44] *Url, W.,* and *F. Gabler:* Mikroskopie 22 (1967) 121

[45] *Vieweg-Gutberlet, F.:* Solid State Electronics, Pergamon Press, Vol. 12 (1969) 731–733

[46] *Wohlmann, A.,* and *R. D. Allen:* J. Cell. Biol. 27 (1965) 116 A

[47] *Wunderer, A.,* and *S. Witte:* ZEISS Information No. 70 (1968) 121